

Post-Column Oxidation of Purpald®-Aldehyde Adducts  
at Nickel Oxide Electrodes

by

Tamara Kerr Mowry

Submitted in Partial Fulfillment of the Requirements  
for the Degree of  
Master of Science  
in the  
Chemistry  
Program

*[Faint signatures and dates are visible in this section, including dates like 5/31/95 and 6/2/95.]*

YOUNGSTOWN STATE UNIVERSITY

JUNE, 1995

Post-Column Oxidation of Purpald®-Aldehyde Adducts  
at Nickel Oxide Electrodes

Tamara Kerr Mowry

I hereby release this thesis to the public. I understand this thesis will be housed at the Circulation Desk of the University library and will be available for public access. I also authorize the University or other individuals to make copies of the thesis as needed for scholarly research.

Signature:

Tamara Kerr Mowry 6/1/95  
Student Date

Approvals:

James H. Milk 5/31/95  
Thesis Advisor Date

Dayl W. Murr 5/31/95  
Committee Member Date

Leonard B. Spiegel 5/31/95  
Committee Member Date

Pat W. Hamrick 6/2/95  
Dean of Graduate Studies Date

## ABSTRACT

Purpald<sup>®</sup>, (4-amino-3-hydrazino-5-mercapto-1,2,4-triazole), a chromogenic agent for detection of aldehydes has been studied as a possible aid for enhancing detectability of aldosterone, as well as simpler aldehydes. Purpald<sup>®</sup> forms a colorless adduct with aldehydes and, after air oxidation another highly colored adduct is formed. An oxidative post-column electrochemical reactor has been investigated as a possible alternative to air oxidation. Optimal operating conditions for reaction time, reaction temperature, pH, and concentration were examined.

## ACKNOWLEDGEMENTS

I would like to thank Dr. James Mike, my advisor, for his time, patience, guidance throughout this research. I would also like to thank Dr. Daryl Mincey and Dr. Leonard Speigel for the time they contributed in reading this thesis.

I thank my husband for his never ending support and encouragement throughout this project.

I would also like to thank Mr. Ted Yurek for doing an outstanding job polishing my nickel electrodes.

## DEDICATION

To my ever patient and understanding husband who suffered through many nights of pizza and subs during the past few years. And to my parents, my in-laws and all of my friends who kept me going and would not let me stop.

LIST OF SYMBOLS	viii
LIST OF FIGURES	1
LIST OF TABLES	iii
CHAPTER	
I. INTRODUCTION	1
A. Oxidation Mechanism of Glucal Electrodes	2
B. Biochemistry of Glucosylated	4
C. Current Methods of Analysis	7
D. Statement of the Problem	8
E. Cyclic Voltammetry	9
F. Spectroelectrochemistry	14
G. Chronoamperometry	17
II. REVIEW OF LITERATURE	26
A. Glucose Analysis by HPLC	26
B. Glucose Analysis by HPLC	28
III. MATERIALS AND METHODS	31
A. Solvents and Reagents	31
B. Electrochemical Studies	32
C. Chronoamperometric Studies	34
D. Electrochemical Sensor Design	36

## TABLE OF CONTENTS

	PAGE
ABSTRACT .....	iii
ACKNOWLEDGEMENTS .....	iv
TABLE OF CONTENTS .....	vi
LIST OF SYMBOLS .....	viii
LIST OF FIGURES .....	x
LIST OF TABLES .....	xii
CHAPTER	
I. INTRODUCTION .....	1
A. Oxidation Mechanism of Nickel Electrodes .....	1
B. Biochemistry of Aldosterone .....	4
C. Current Methods of Analysis .....	7
D. Statement of the Problem .....	8
E. Cyclic Voltammetry .....	9
F. Spectroelectrochemistry .....	14
G. Chromatography.....	17
II. REVIEW OF LITERATURE .....	26
A. Aldehyde Analysis by HPLC .....	26
B. Aldosterone Analysis by HPLC .....	29
III. MATERIALS AND APPARATUS .....	31
A. Solvents and Reagents .....	31
B. Electrochemical Studies .....	32
C. Chromatographic Studies .....	35
D. Electrochemical Reactor Design ....	36

IV.	RESULTS AND DISCUSSION .....	43
A.	Electrochemical Characterization .....	43
B.	Spectroelectrochemical Characterization .....	48
C.	Optimizing Chromatographic Conditions .....	52
V.	CONCLUSION AND SUGGESTIONS FOR FUTURE WORK .....	66
A.	Suggestions for Future Work .....	66

## LIST OF SYMBOLS

SYMBOLS	DEFINITION
HPLC	High Performance Liquid Chromatography
NPLC	Normal Phase Liquid Chromatography
RPLC	Reverse Phase Liquid Chromatography
TLC	Thin-Layer Chromatography
LSC	Liquid-Solid Chromatography
LLC	Liquid-Liquid Chromatography
BPC	Bonded-Phase Chromatography
IEC	Ion Exchange Chromatography
RIA	Radioimmunoassay
GC	Gas Chromatography
GC-MS	Gas Chromatography-Mass Spectrometry
MS	Mass Spectrometry
ODS	Octadecylsilane
OTE	Optically Transparent Electrode
DNPH	2,4 - Dinitrophenyl Hydrazine
CDB	2-(4-Carboxyphenyl)-5,6-dimethyl- benimidazole
DMB	1,2-Diamino-4,5-methylenedioxybenzene
UPH	Ultra High Purity
m	meter
cm	centimeter



mm	millimeter
nm	nanometer
$\mu\text{m}$	micrometer
ppt	parts-per-thousand
$\mu\text{g}$	microgram
pg	picogram
dL	deciliter
M	molarity
Å	angstrom
V	volts
E	potential
i	current
$\epsilon$	molar absorptivity
$\approx$	approximately
$R_s$	resolution
$t_r$	retention time
$^{\circ}\text{C}$	degrees Celcius
psi	pounds per square inch

14.	Schematic Diagram of Electrochemical Reactor A	40
15.	Schematic Diagram of Electrochemical Reactor B	41
16.	Schematic Diagram of Electrochemical Reactor C	42
17.	Cyclic Voltammogram of Working Electrode in NaOH	43
18.	Cyclic Voltammogram of Supporting Electrolyte	46
19.	Cyclic Voltammogram After Addition of Aldosterone	47

## LIST OF FIGURES

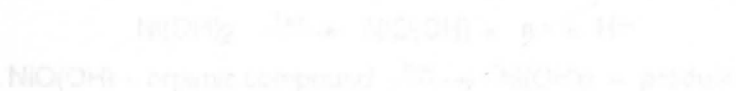
FIGURE	PAGE
1. Reaction Mechanism of Purpald .....	2
2. Cyclopentanoperhydrophenanthrene .....	4
3. Aldosterone .....	5
4. Equilibrium forms of Aldosterone .....	5
5. Triangular Waveform .....	11
6. Typical Voltammogram .....	11
7. Irreversible and Reversible Voltammograms .....	13
8. Typical Spectroelectrochemical Cells .....	16
9. Schematic Representation of the Chromatographic Process .....	23
10. A Typical Chromatogram .....	24
11. Resolution in Liquid Chromatography .....	25
12. Spectroelectrochemical Cell .....	34
13. Schematic Drawing of the HPLC System .....	37
14. Schematic Drawing of Electrochemical Reactor A .....	40
15. Schematic Drawing of Electrochemical Reactor B .....	41
16. Schematic Drawing of Electrochemical Reactor C .....	42
17. Cyclic Voltammogram of Nickel Electrode in NaOH .....	45
18. Cyclic Voltammogram of Supporting Electrolyte .....	46
19. Cyclic Voltammogram After Addition of Aldosterone .....	47

20.	Spectroelectrochemical Examination of Oxidation of Purpald .....	51
21.	Oxidation of Formaldehyde Using Electrochemical Reactor A .....	54
22.	Oxidation of Formaldehyde Using Electrochemical Reactor B .....	55
23.	Oxidation of Formaldehyde Using Electrochemical Reactor C .....	56
24.	Effect of Flow Rate on Detector Response for Formaldehyde .....	61
25.	Effect of Applied Potential on Detector Response for Formaldehyde .....	62
26.	Effect of Temperature on Detector Response for Formaldehyde .....	63
27.	Effect of Temperature on Detector Response for Acetaldehyde .....	64
28.	Effect of Molecular Weight Increase on Detector Response .....	65

## LIST OF TABLES

TABLE	DESCRIPTION	PAGE
1.	Reaction Time for Formation of Purple Purpald®-Aldehyde Complex .....	49

The use of nickel electrodes in alkaline medium under conditions of reductive electrocatalysis has been reported in various papers for the electrocatalytic oxidation of carbohydrates (1-3), sugars and sugar degradation products (4,5), amino acids and alcohols (6,7). It has been shown by Fleischman (8) and others that when a nickel electrode is in contact with an alkaline solution the surface is spontaneously covered by a layer of nickel(II) hydroxide, which in turn can be oxidized to a nickel(III) oxide/hydroxide layer whose structure is strongly dependent on the applied potential (9), and temperature (10). The nickel(III) surface acts as a strong oxidant and can react with organic compounds such as carbohydrates. As a result, the nickel(III) is reduced to nickel(II) hydroxide, which can be oxidized by the applied potential to give the analytical signal (11). Fleischman and his colleagues have proposed the following mechanism for the catalytic oxidation of an organic compound at a nickel electrode:

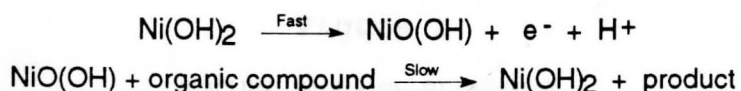


## CHAPTER I

## INTRODUCTION

A. Oxidation Mechanism of Nickel Electrodes

The use of nickel electrodes in alkaline medium had been cited in numerous papers for the anodic oxidation of carbohydrates [1-4], sugars and sugar degradation products [5-6], and amines and alcohols [7]. It has been shown by Fleischman [8] and others that when a nickel electrode comes in contact with an alkaline solution the surface is spontaneously covered by a layer of nickel(II) hydroxide, which in turn can be oxidized to a nickel(III) oxide/hydroxide layer whose structure is strongly dependent on the applied potential, pH, and temperature [4]. The nickel(III) surface acts as a strong oxidant and can react with organic compounds such as carbohydrates. As a result, the nickel(III) is reduced to nickel(II) hydroxide, which can be oxidized by the applied potential to give the analytical signal [9]. Fleischmann and his colleagues have proposed the following mechanism for the catalytic oxidation of an organic compound at a nickel electrode.



The fact that the nickel(III) oxide is a strong oxidant and is generated at the electrode surface was the basis for this work. Rather than using the nickel electrode directly for amperometric detection of organic molecules, which is typical, the nickel surface served as an oxidizing agent after the separation of aldehydes by HPLC. However, the direct oxidation of the carbonyl group on the aldehyde was not investigated. Instead the aldehydes were derivatized with the chromogenic reagent as they exited the chromatography column.

The derivatizing agent 4-amino-3-hydrazino-5-mercapto-1,2,4-triazole, commercially known as Purpald®, has been used for a number of years to visualize carbohydrates in spot tests in thin layer chromatography (TLC) and as a reagent for carbonyl group analysis [10]. The mechanism by which Purpald® reacts with compounds possessing an aldehyde functional group is shown below.

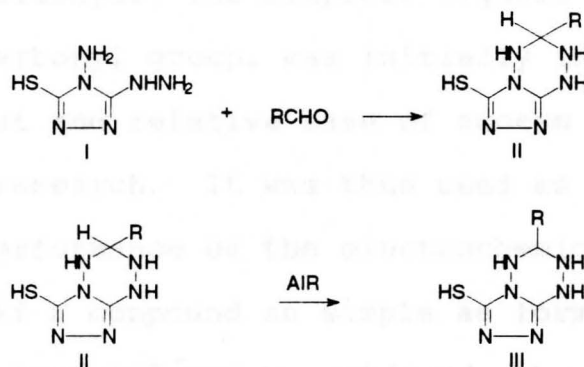


**Figure 1**

REACTION MECHANISM OF PURPALD®

The triazole (I) condenses with the aldehyde to form an unstable, oxygen labile, intermediate (II) [11]. Air oxidation of this intermediate leads to the formation of a purple, intensely colored, bicyclic, heterocyclic, 6-mercapto-3-substituted-s-triazole[4,3-b]-s-tetrazine (III). This highly conjugated double-bond system allows for spectroscopic detection in the visible wavelength region.

Under chromatographic conditions the mobile phases are usually degassed with an inert gas. As a result very little if any dissolved oxygen is present in the system. Since air is the oxidant for this reaction and is of vital importance to drive the second step, an alternative method of oxidation was required. This was the role of the nickel electrode. As stated previously nickel(III) oxide is a powerful oxidant, it was hoped that the oxidation step required to drive the reaction to completion could be accomplished at the nickel electrode surface.

Formaldehyde, the simplest organic compound containing a carbonyl group, was initially investigated because its cost and relative ease of access made it ideal to begin this research. It was thus used as a guide to evaluate the performance of the electrochemical cell. It was felt that if a compound as simple as formaldehyde would not react with Purpald® and be oxidized, then most likely aldehydes with higher molecular weights would not be oxidized. As stated earlier, the ultimate goal of this work

was to develop a new, sensitive, and reliable approach for detection of aldosterone in urine and blood by HPLC.

### B. Biochemistry of Aldosterone

Of the more than three dozen hormones produced by the adrenal cortex only seven are known to have direct effects upon body functions [12]. These corticosteroids, as they are commonly referred to, are grouped into three classes.

1. Glucocorticoids
2. Mineralcorticoids
3. Androgens or Sex Hormones

While each of the groups of hormones have very different functions they do possess a basically similar structure. They are derivatives of cholesterol and contain the cyclopentanoperhydrophenanthrene nucleus [13].

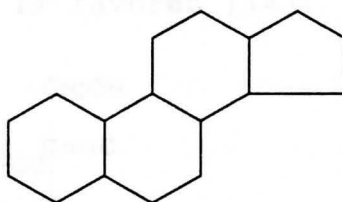


**Figure 2**

CYCLOPENTANOHYDROPHENANTHRENE  
NUCLEUS



Aldosterone is classified functionally as a mineralocorticoid because its main action concerns mineral salt (electrolyte) metabolism. The structure of aldosterone, ( $\Delta^4$ -Pregnen-18-al-11 $\beta$ ,21-diol-3,20-dione-(11 $\rightarrow$ 18)-lactol), as seen in Figure 3 [14], was first determined by Simpson, Tait, Wettstein, Neher, vonEuw, Schnidler, and Reichstein in 1954 [15].

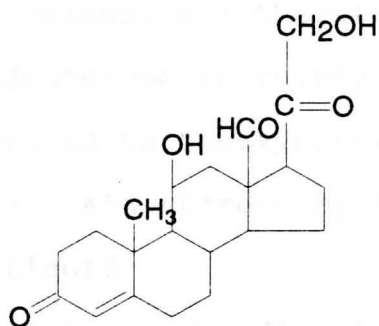


**Figure 3**

ALDOSTERONE

In solution aldosterone exists in equilibrium between the aldehyde structure and the hemiacetal. The hemiacetal structure is favored [14].

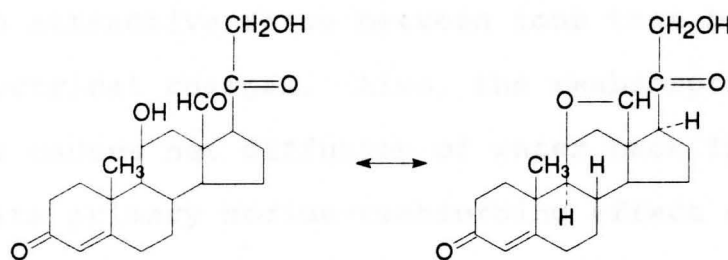


**Figure 4**

ALDOSTERONE

HEMIACETAL

The primary and general function of the mineralocorticoids seems to be to maintain homeostasis of the blood concentration of sodium [16]. In doing this, these hormones also help to maintain a normal ratio of blood sodium concentration to potassium concentration and normal volumes of extracellular and intracellular fluids. In short, mineralocorticoids play a crucial part in maintaining electrolyte and fluid balance and therefore in maintaining healthy survival. Aldosterone is thirty times more active in these respects compared to desoxycorticosterone, another mineralocorticoid [13]. Aldosterone by far is the most important mineralocorticoid.

Aldosterone acts on the distal renal tubule cells of the kidney, stimulating them to increase their reabsorption of sodium ions from tubule urine back into blood. In exchange for each reabsorbed sodium ion, tubule cells excrete either a potassium ion or a hydrogen ion. Moreover, as each positive sodium ion is reabsorbed, a negative ion either (bicarbonate or chloride) follows along, drawn by the attractive force between ions that bear opposite electrical charges. Also, the reabsorption of electrolytes causes net diffusion of water back into blood. Because of its primary sodium-reabsorbing effect on kidney tubules, aldosterone tends to produce sodium and water retention but potassium and hydrogen ion loss.

The average plasma concentration of aldosterone,

both free and bound, is  $0.006 \mu\text{g}/\text{dL}$ , with an average of  $150 \mu\text{g}/24\text{hr}$ . These values are morning values after an overnight recumbency and are considered normal values [13]. In persons having elevated mineralocorticoid levels a syndrome of primary hyperaldosterism, called Conn's syndrome, exists [17]. These patients are severely  $\text{K}^+$  depleted and are hypertensive. Prolonged  $\text{K}^+$  depletion damages the kidneys, however this condition can be treated once the levels of aldosterone are determined.

### C. Current Method of Analysis

Radioimmunoassay (RIA) remains the most widely accepted method of analysis for urinary and plasma aldosterone determinations [18]. In one method, aldosterone-3-carboxymethoxime-18,21-diacetate is coupled with rabbit albumin and antibodies are produced in rabbits.  $1,2\text{-}^3\text{H}$ -aldosterone is then added to the sample for radioactive measurements [19]. The  $^3\text{H}$ -aldosterone antibody complex is measured using a liquid scintillation counter.

Another method, described by Bennett [20], is one developed by Diagnostic Products Corporation (Los Angeles, CA), in which aldosterone is tagged with radioactive iodine,  $^{125}\text{I}$ , rather than  $1,2\text{-}^3\text{H}$ -aldosterone. Competition between endogenous aldosterone and radioactive labeled aldosterone for an aldosterone specific antibody takes place.

Separation of free aldosterone from the bound portion is possible by using dextran coated charcoal. The radioactivity in either the bound or unbound portion is counted and the counts per minute are compared to known standards. For a more indepth study of RIA methods the reader is referred to reference 18.

#### D. Statement of the Problem

The physiological importance of aldosterone can not be overstated. For this reason having a sensitive, accurate, and rapid analytical procedure to determine plasma and urine levels of aldosterone is a desire of the clinician. The current methodology using radioimmunoassay has numerous drawbacks. The methods are tedious and cumbersome, and consistently good technique is required to get accurate and reproducible results. Large automated multi-isotope measuring instruments are expensive, as are the radioisotopes used for analysis. The radioisotopes tend to have short shelf-lives and are hazardous to work with, as well as being costly for waste disposal.

An alternative would be to develop a method of analysis that uses liquid chromatography. HPLC is used on a regular basis in the clinical setting and is therefore readily available. The method of detection most commonly employed with HPLC is ultra-violet/visible absorption

spectrophotometry. Aldosterone is a strong chromophore with a molar absorptivity value of  $\epsilon \approx 15,000$  at 240 nm, however, there are many 3-keto-steroids present in urine that also absorb at 240 nm and interfere with chromatographic separation of aldosterone, thereby making accurate detection difficult. Aldosterone is unique among the adrenal steroids by having an aldehydic functional group at carbon 18 (Figure 3). It was the objective of this research to develop a method to improve the detectability of aldosterone by using Purpald® as a chromogenic agent that reacted specifically with the aldehyde group and a post-column reactor equipped with a nickel electrode.

#### E. Cyclic Voltammetry

Cyclic voltammetry is a scanning electrochemical technique in which the potential of a solid electrode submerged in a quiescent solution is cycled between two different values. The varying of potentials involves use of a triangular sweep, first in one direction and then in the reverse direction as seen in Figure 5 [21]. The initial potential and the value in which the sweep reverses direction are referred to as the switching potentials. The electrode at which the potential is applied is the working electrode and its potential is controlled relative to a reference electrode. The current flowing through the

working electrode is monitored as a function of the applied potential [22]. The results are displayed as current potential plots known as voltammograms. A typical voltammogram is shown in Figure 6 [21]. The initial potential  $E_1$  is selected well outside of the potential range at which electrolysis would occur for a given analyte. As the potential becomes more negative, current begins to flow until a maximum is reached. At the switching potential  $E_2$ , the scan direction is reversed and becomes more positive. The potential at which current begins to flow is directly related to the amount of energy needed to initiate the oxidation or reduction of a chemical species at or near the surface of the working electrode. The observed current is the response signal and the energy, or potential, is the excitation signal. The resulting voltammogram is a plot of the relationship that exists between the current and potential for a particular chemical species.

A cyclic voltammogram can indicate important information with regard to a particular redox system. The magnitude of the anodic peak  $(i_p)_a$  current, the cathodic peak  $(i_p)_c$  current, the anodic peak potential  $(E_p)_a$ , the cathodic peak potential  $(E_p)_c$ , and the half-peak potential  $(E_{p/2})_c$  can be measured. Extrapolation of the baseline is necessary for correct measurement of  $i_p$ .

When both species of a redox couple exchange electrons quickly with the working electrode the reaction is

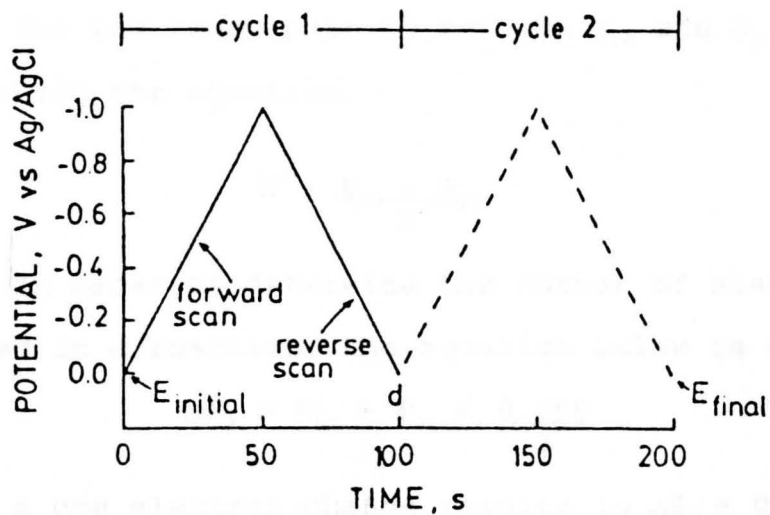


Figure 5

Triangular potential waveform with switching potentials at 0.0 V and -1.0 V versus Ag/AgCl [21]

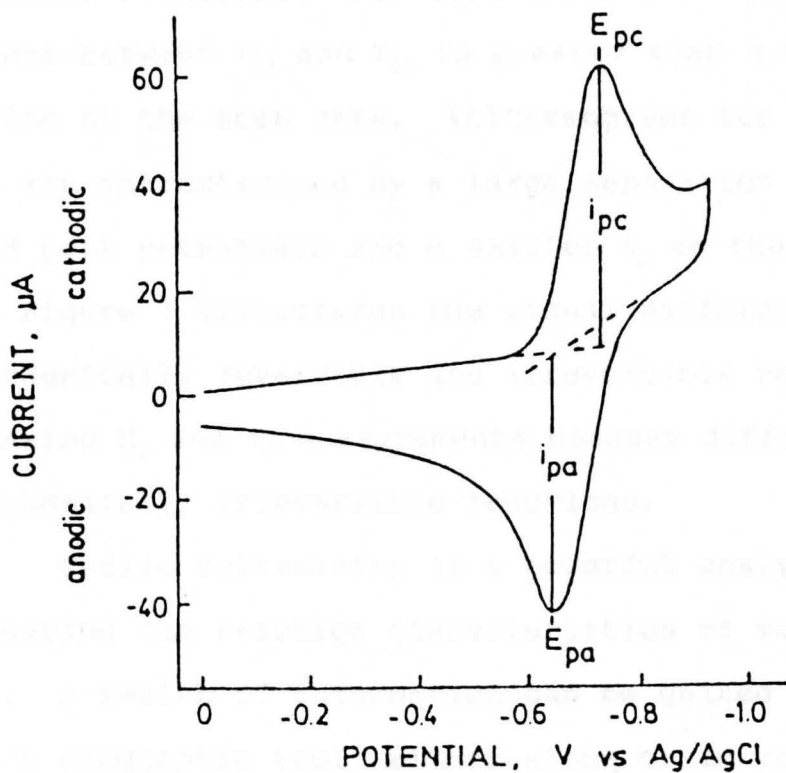


Figure 6

Typical Voltammogram [21]

said to be electrochemically reversible. The formal potential for the redox pair is between  $E_{pa}$  and  $E_{pc}$  and is found by using the equation.

$$E^{\circ'} = \frac{E_{pa} + E_{pc}}{2} \quad [23]$$

In order to determine the number of electrons transferred in a reaction, the equation below is used.

$$\Delta E_p = E_{pa} - E_{pc} = \frac{0.059}{2}$$

A one electron change results in  $\Delta E_p = 0.059$  V. For a truly reversible reaction, the values for  $i_{pa}$  and  $i_{pc}$  should be equal regardless of the scan rate. The same statement does not hold true for electrochemically irreversible reactions. For irreversible reactions the difference between  $E_{pa}$  and  $E_{pc}$  is greater than 0.059 V and is a function of the scan rate. Voltammograms for irreversible systems are characterized by a large separation in the observed peak potentials and a smaller  $i_p$  on the reverse scans. Figure 7 illustrates the visual differences between electrochemically reversible and irreversible reactions [23]. Making  $E_p$  and  $i_p$  measurements becomes difficult with electrochemically irreversible reactions.

Cyclic voltammetry is a powerful analytical method for measuring the reaction characteristics of various redox systems. A wealth of information can be gained when it is used as a diagnostic tool, either alone or in conjunction with other techniques such as spectroscopy.



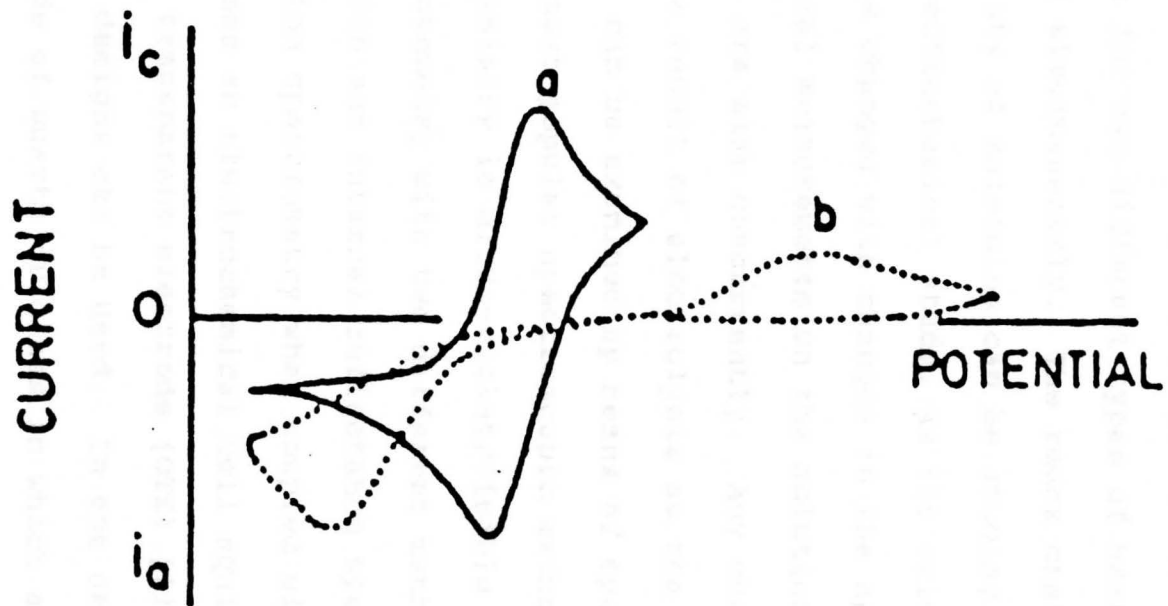


Figure 7

Cyclic Voltammogram exhibiting electrochemical:  
(a) reversibility (b) irreversibility [23]

## F. Spectroelectrochemistry

Spectroelectrochemistry, as described by Heineman, involves the combination of an electrochemical technique with a spectroscopic technique [24]. The advantage of the coupling of these two techniques is that it allows for two different types of measurements to be performed simultaneously. The redox characteristics of a wide variety of molecules can be studied. In a spectroelectrochemical study, as the oxidation state of the analyte is changed with changes in the applied potential, the spectral measurements on the solution adjacent to the electrode are made concurrently. Any chemical changes that occur as a result of electrolysis at the solution-electrode interface can be examined by means of spectroscopy.

The most popular spectroscopic method used with electrochemistry is ultra-violet/visible absorption spectrophotometry with two different methods available - transmission and internal reflectance spectrophotometry. Transmission spectrometry when coupled with electrochemical methods uses an electrochemical cell equipped with an optically transparent electrode (OTE) [23]. Two different electrode designs can be used. In one design the electrode can be made of quartz or glass in which a very thin film of conductive material such as gold, platinum, carbon, or tin oxide has been applied to the surface. The film thickness

is in the range of 100 - 5000 Å. The transparency of these electrodes is 20 - 85 %T [24].

An alternate design of an OTE uses a metal micro-mesh screen of either gold, silver, nickel, or copper. The holes in the screen allow the optical beam to pass through the solution and electrode to the detector without significantly obstructing the signal. The screens usually have 100 - 2000 wires/inch and are useful over a large spectral wavelength range. The transparency of these electrodes is comparable to the thin film OTE [25]. The micromesh screens have the same electrochemical properties as larger, more conventional, electrode materials. The potential ranges in which the electrodes operate are identical.

The electrochemical cells for internal reflectance spectrophotometry are similar to those used for transmission spectrometry. However, instead of the beam passing through the OTE, the optical beam is focused on the back of the OTE. The beam is totally reflected if the incident angle is greater than the critical angle. The solution adjacent to the electrode is monitored.

Cell construction can take on many forms, however the most common is the sandwich type, two examples are shown in Figure 8 [22]. The design of this type of cell is simplistic in its construction, flexible in allowing for changes in the OTE as well as introduction of auxillary and

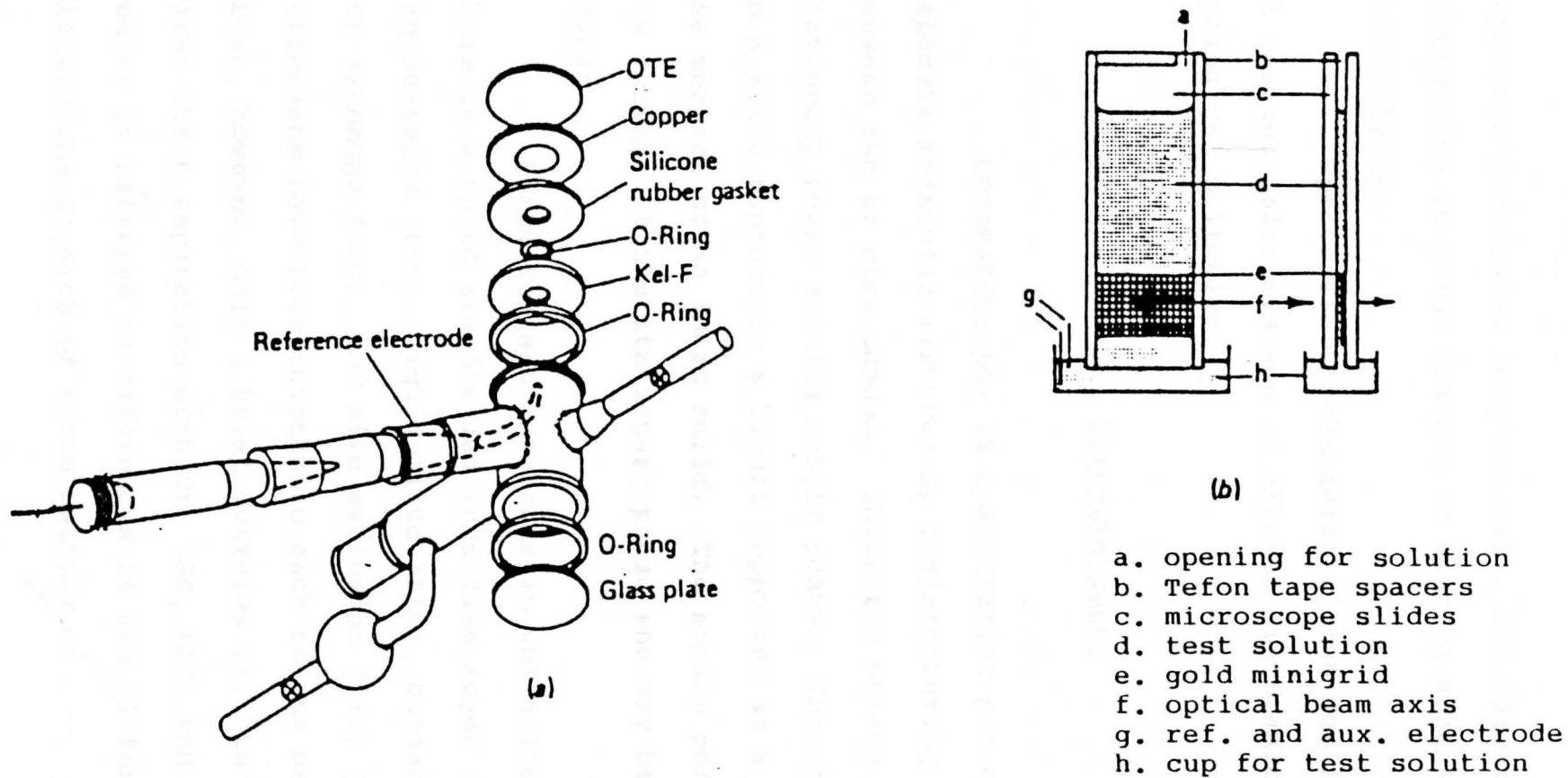


Figure 8

Cells for Transmission Spectroelectrochemistry

reference electrodes into the cell, and convenient for determining spectral changes in species generated by electrolysis.

Spectroelectrochemistry allows for in-depth study of various redox systems of organic, inorganic, and biological molecules.

### G. Chromatography

Chromatography is a separation process used to separate molecular mixtures by redistributing molecules between two or more phases. These two phases are called the stationary phase and the mobile phase. The stationary phase is a solid support or a liquid supported as a thin-film on the surface of an inert solid. The mobile phase flows over the surface of the stationary phase and may be gas or liquid.

Chromatographic methods in which the stationary phase is a solid are divided into five major categories: liquid-solid (LSC), liquid-liquid (LLC), bonded phase (BPC), ion exchange (IEC), and size exclusion (SEC) [27]. Numerous monographs have been devoted to each of the methods listed above, however, only a brief overview will be given for the first three separation methods, LSC, LLC, and BPC. The reader is referred to references 26 and 27 for more detailed discussions on each of these methods.

In liquid-solid chromatography (LSC) the mode of separation is by adsorption. LSC relies on the distribution of the components of a mixture to be separated between a bulk fluid, the liquid mobile phase, and a solid stationary support phase. Solvent molecules in the mobile phase compete with solute molecules for sites on the adsorbent. In order for the solute molecules to be adsorbed on to the stationary phase a solvent molecule must first be displaced from the surface. If the adsorbent possesses a polar surface such as silica or alumina, non-polar groups will have little affinity for the surface and will not displace the solvent molecules, therefore they will not be retained. A feature of liquid-solid chromatography is the degree of selectivity that can be introduced in to the technique. LSC is less sensitive to molecular weight variations between solute species but very sensitive to the type of compound being separated.

Liquid-liquid chromatography (LLC) or partition chromatography involves a liquid stationary phase, which is dispersed on to a finely divided inert support material, and a liquid mobile phase. The sample to be analyzed is mixed in the mobile phase and is partitioned between the mobile phase and the stationary phase according to its partition coefficient  $K$  [26]. This partitioning leads to a differential rate of migration and separation occurs. As the name implies for LLC both phases are liquid, as in

solvent extraction, and therefore they must be immiscible in each other [27]. However, since the sample must be soluble in both the mobile phase and stationary phase it follows that these two liquid phases must be mutually soluble to some degree. As a result of this mutual solubility the stationary phase is gradually stripped off of the inert solid support by the mobile phase. When this occurs the column performance begins to deteriorate. The advent of chemically bonded stationary phases has reduced this problem.

Bonded phase chromatography (BPC) in principle is similar to liquid-liquid chromatography, however, BPC utilizes stationary phases in which the liquid phase has been chemically bonded to silica gel or a polymeric resin surface by Si-O-R linkages. The organic group, R, is held in place on the stationary phase surface through covalent bonding. These liquid bonded-phases are highly stable and are not easily removed as those used for liquid stationary phases in LLC.

The selectivity of the bonded phase can be changed by varying the polarity of the liquid phase with changes in the R group. The most common organic group used is an alkyl chain with 18 carbon groups. Stationary phases with this functional group affixed to the surface tend to be non-polar. By shortening the chain length of the alkyl group, the polarity of the surface changes. These R groups are

referred to as *ligates* [27]. Other ligates that are often bonded to the stationary support are phenyl, methoxy, amino, and diamino. Bonded-phase chromatography has become the most widely used method of liquid chromatography to date.

The terms normal phase and reverse phase are used when discussing liquid chromatographic processes. The term normal phase arose from the early use of silica gel as a stationary phase during the advent of liquid chromatography. It became the standard to label LSC methods using silica gel as normal phase LC (NPLC). Today this phrase refers to liquid chromatographic methods that use a polar stationary phase to separate components of a mixture while using a non-polar liquid mobile phase. The term reversed phase LC (RPLC) refers to the opposite situation, the stationary phase is non-polar and the liquid mobile phase is polar. Separation methods for LSC, LLC, and BPC can be either normal phase or reversed phase, however, most of the literature published today refers to reversed phase liquid chromatography (RPLC).

In HPLC the various components of a mixture are carried through a chromatographic column packed with stationary phase by the mobile phase. The stationary phase is a solid support, such as silica or resin beads, with a very small particle size, characteristically 3 - 5  $\mu$ , that may nor may not be chemically modified. The mobile phase and sample move through the column with the aid of high



pressure pumps. As the mixture moves through the column the individual components begin to partition between the mobile phase and the stationary phase at different rates depending on the relative affinity of the individual solutes for each phase. The sorption - desorption process occurs rapidly as the mixture travels the length of the column and approximates equilibrium. As time passes, the mixture is separated and the individual components appear at the column outlet and the detector at various times referred to as retention times,  $t_r$  [26]. Retention time is a measure of the time from when the sample was injected until a solute band leaves the column. This process is depicted in Figure 9. The resulting plot, called a chromatogram, is a record of the separation (Figure 10) [22].

A chromatogram is a representation of time versus detector response. The detector signal appears as a peak on the chromatogram representing a mirror image of the frequency distribution of each solute as it travels through the column. The ideal chromatographic peak is Gaussian shaped with the peak maximum corresponding to the retention time. This value is characteristic of a solute and may be used as one method of identification when separating a mixture. A repeated injection of the same analyte will have the same retention time. The area under the peak is proportional to the concentration.

The chromatogram pictured in Figure 11 shows

complete separation between all of the peaks. The degree of separation of two solute peaks is referred to as the resolution ( $R_s$ ), [27]. Resolution can be determined directly from the chromatogram and is expressed mathematically by the equation below,

$$R_s = \frac{t_2 - t_1}{\frac{1}{2}(t_{w1} + t_{w2})} \quad [27]$$

where  $t_1$  and  $t_2$  refer to the  $t_r$  values of bands 1 and 2 and  $t_{w1}$  and  $t_{w2}$  are their band width. Large  $R_s$  values indicate good separation whereas smaller  $R_s$  values indicate poor separation, which makes quantitation difficult or impossible. A minimum peak resolution of 1.0 is required to do quantitative analysis.

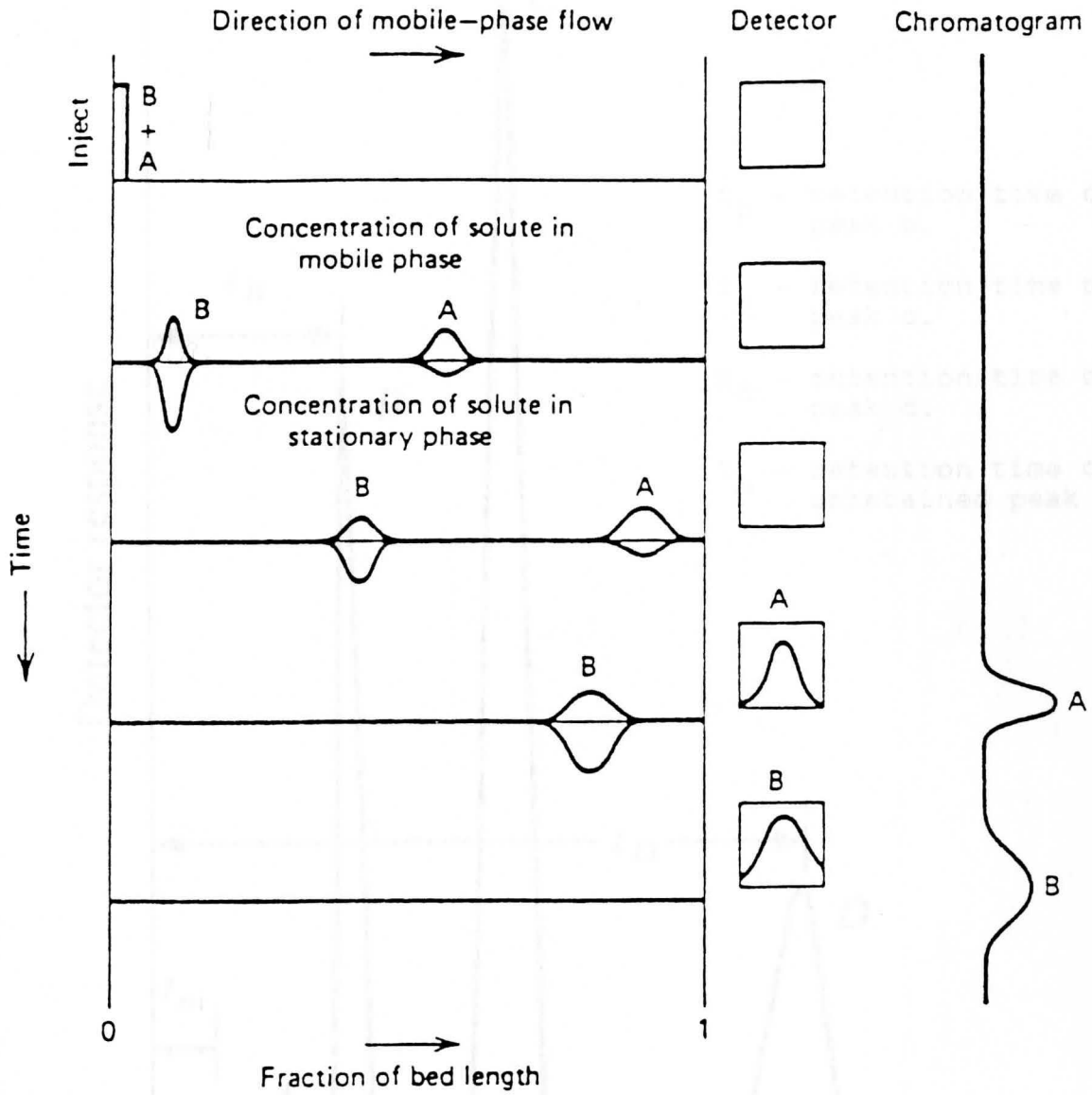


Figure 9

Schematic Representation of the Chromatographic Process [26]

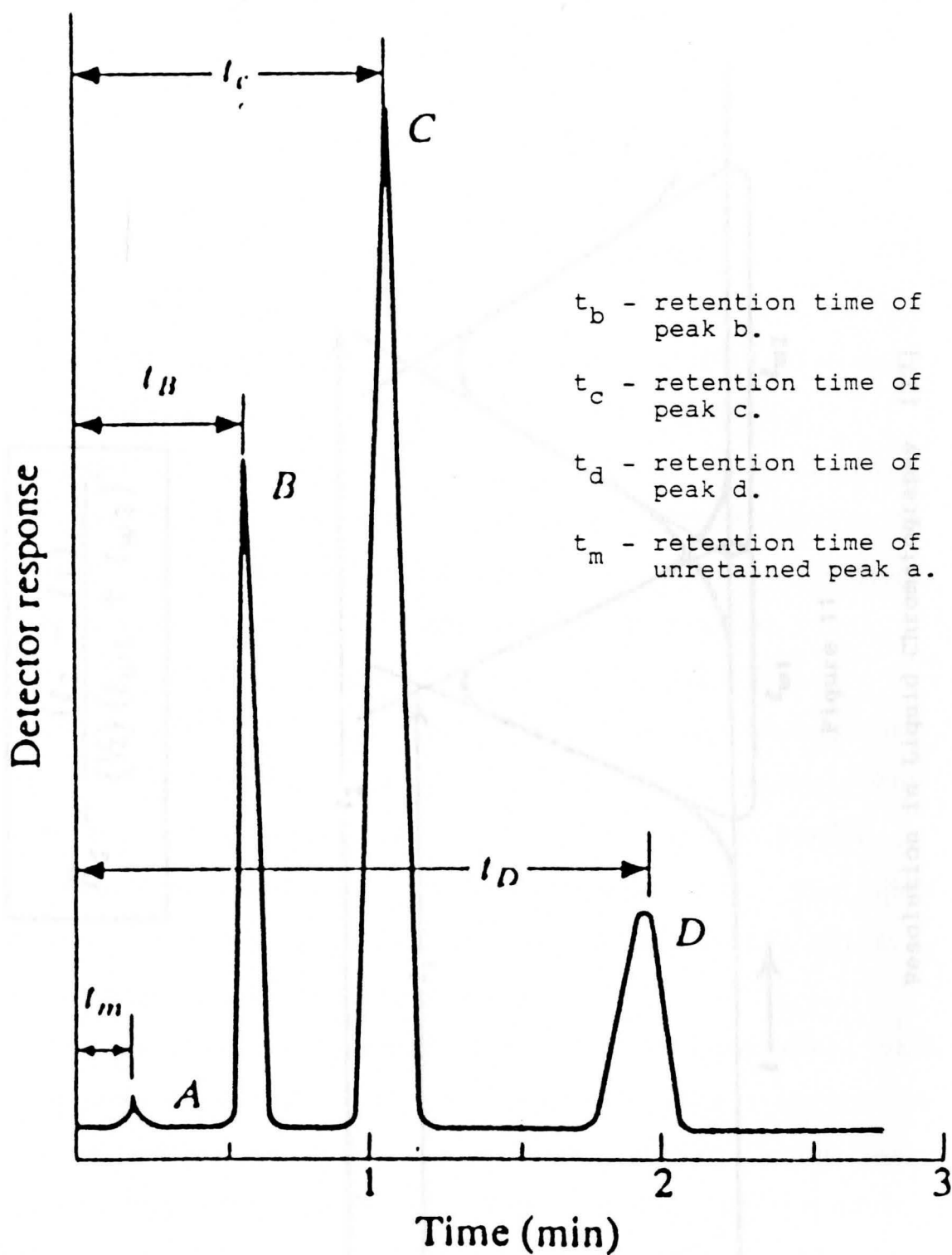


Figure 10

Typical Chromatogram [22]

$$R_s = \frac{(t_2 - t_1)}{(\frac{1}{2})(t_{w1} + t_{w2})}$$

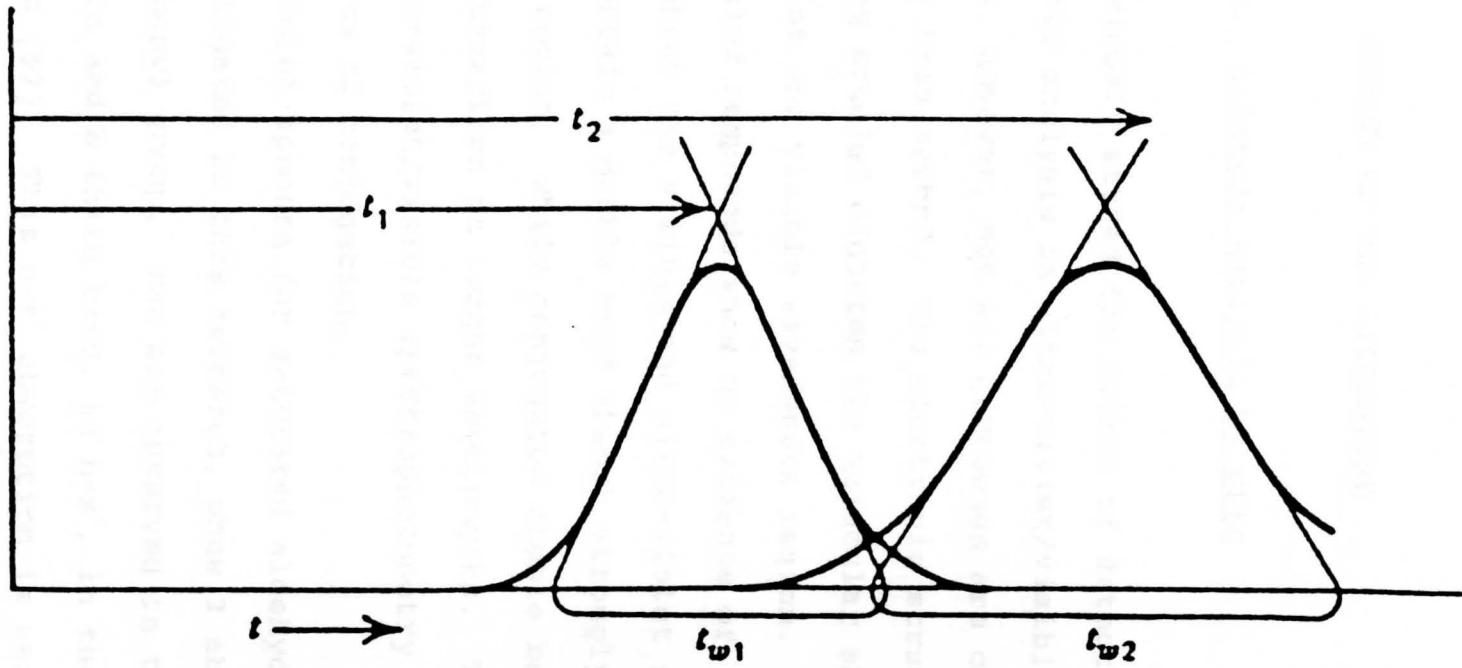


Figure 11

Resolution in Liquid Chromatography [27]

## CHAPTER II

## REVIEW OF THE LITERATURE

A. Aldehyde Analysis by HPLC

As previously stated the method of detection most often used for HPLC analysis is ultra-violet/visible spectrophotometry, however, not all compounds are capable of being detected by this method. The electronic structure of the molecule being studied dictates the molecular absorption in the ultra-violet and visible wavelength region. Completely saturated compounds show no evidence of absorption throughout the visible and ultra-violet regions. Compounds that contain a double bond absorb strongly in the far ultra-violet region, while conjugated double bonded systems produce absorption at longer wavelengths. The ideal molecule for ultra-violet/visible spectrophotometry would possess some degree of conjugation.

Ultra-violet spectra for saturated aldehydes, such as the ones investigated in this research, show 3 absorption bands for the carbonyl group. Two are observed in the far ultra-violet region and a third band, an  $n \rightarrow \pi^*$ , in the near ultraviolet region [52]. This  $n \rightarrow \pi^*$  absorption is weak ( $\epsilon_{\max} < 30$ ). Derivatizing the aldehydes with an reagent that

possesses a high level of conjugation would result in a increase in molar absorptivity and a shift to a longer wavelength thereby improving detection.

Most of the derivatives that have been used for gas chromatography (GC), gas chromatography/mass spectrometry (GC-MS), mass spectrometry (MS), and high performance liquid chromatography (HPLC) analysis of aldehydes and ketones stem from the classical carbonyl derivatives such as phenylhydrazones and dinitrophenyl hydrazones as well as oximes. The dinitrophenyl hydrazones have been found useful for chromogenic derivatization for HPLC analysis [28,29,30]. The current methods of analysis utilize 2,4-dinitrophenyl hydrazine (DNPH) with electrochemical detection. Chiavari and Bergamini [31] described a method in which carbonyl compounds present in acid rain were derivatized using DNPH. The separation was done using an Erbasil C<sub>18</sub> reversed-phase column. The mobile phase was prepared from triply distilled water and methanol (30:70) and contained a supporting electrolyte of 1 g/L LiClO<sub>4</sub> and 0.05 g/L H<sub>2</sub>SO<sub>4</sub>. Detection was achieved using a glassy carbon electrode. The optimum potential was approximately +1.10 V versus a Ag/AgCl reference electrode. Detection limits for formaldehyde were as low as 30 pg.

HPLC analysis of aldehydes has also been described using 3-methylbenzothiazolone as a derivatizing agent with electrochemical detection at a glassy carbon electrode

[32,33]. Analysis of atmospheric formaldehyde as its lutidine derivative, followed by HPLC with spectrophotometric detection, has been performed by the same author [34]. Also three methods of reductive amination have been investigated by Mann and Grayeski for derivatization of aldehydes and ketones using 3-aminofluoranthene as a chemiluminescence agent [35].

Of particular interest for this research was work done by Del Nozal and co-workers [10]. Purpald<sup>®</sup> was used as a post-column derivatizing agent for monosaccharides. The reagent phase contained 4.0 ppt Purpald dissolved in 2 M NaOH. The monosaccharides were separated using an Aminex HPX-87P cation-exchange column at 85°C. A 20 m mixing coil provided the time for the chemical derivatization reaction to go to completion. The mixing coil was kept at 90°C in a constant temperature water bath. Immediately after the heated bath the eluant was cooled in an ice bath. The derivatized product was detected at 550 nm using a UV-Visible spectrophotometric detector. A 0.04 M solution of H<sub>2</sub>O<sub>2</sub> served as the oxidant.

The optimum concentration for the NaOH was found to be ≈1 M. This was determined by plotting the maximum absorbance of formaldehyde versus NaOH concentration. Del Nozal found the optimum concentration of the Purpald<sup>®</sup> to be 0.01 M. The temperature was also critical for the reaction time. The results were very promising and very applicable to this research.



## B. Aldosterone Analysis by HPLC

As previously mentioned radioimmunoassay is the most widely accepted method for determining aldosterone levels in urine and plasma. In recent years, however, the use of high performance liquid chromatography had been investigated as either an alternative method of analysis or has been used in conjunction with RIA methods. In a study by Ueshida et al. [36] a method for simultaneously measuring steroid hormone levels in serum, they described the use of HPLC coupled with RIA. Twelve different tritium-labeled steroids, including aldosterone, were separated using HPLC with fractions of the column eluant collected. The concentration of the eluant fractions were then quantified using RIA. The results of this method correlated well with those obtained from conventional  $^{125}\text{I}$  RIA methods.

Another approach for measuring aldosterone in plasma was using pre-column derivatization with 2-(4-carboxyphenyl)-5,6-dimethylbenzimidazole (CDB). Katayama and co-workers [37] derivatized eight corticosteroids with CDB to their corresponding esters. The esterification reaction was enhanced by the addition of 4-piperidino-pyridine, which acted as a catalyst while 1-isopropyl-3-(3-dimethylaminopropyl)carbodiimide perchlorate served as the esterification reagent. Use of these compounds had a significant effect on detector response. After solid-phase

extraction using a C<sub>18</sub> solid phase extraction cartridge, the CDB esters were separated by HPLC on an ODS reversed-phase column with a water-methanol mobile phase. Detection of the derivatized compounds was using fluorescence spectroscopy with excitation at 334 nm and emission at 418 nm. The detection limits for the steroids ranged from 0.06 - 0.3 pg per 100  $\mu$ L of plasma.

Yoshitake, Hara, Yamaguchi and Nakamura [38] also used fluorimetric detection to assay corticosteroids with 1,2-diamino-4,5-methylenedioxybenzene (DMB). The hormones were first oxidized by cupric acetate to form the corresponding glyoxal compounds, which were then derivatized with DMB. The derivatives were separated chromatographically using a TSK gel ODS-120T column with gradient elution by mixtures of methanol, acetonitrile and 1.0 M ammonium acetate. The excitation and emission wavelengths were 350 nm and 390 nm respectively. The recovery rate of aldosterone added to human serum was  $99.9 \pm 5.9\%$ .

## CHAPTER III

## MATERIAL AND APPARATUS

A. Solvents And Reagents

All chemicals and solvents used were reagent grade or of the highest purity available.

Doubly deionized and ultra-filtered water was used for the preparation of all reagent and solvent systems.

Solvents and reagents were prepared or used as described below.

HPLC grade acetonitrile (Fisher Scientific, Pittsburgh, Pa.) was ultra-filtered through nylon filters with a pore size of 0.45 micron (Micron Separations, Inc.).

Sodium hydroxide pellets were used to prepare a 1.0 N solution.

Sodium perchlorate was used to prepare a 0.2 M solution.

Purpald® (Sigma Chemical Co., St. Louis, MO) was used in its pure form and also to prepare 0.05 M and 0.1 M solutions.

UHP Helium (Mahoning Valley Welding, Youngstown, OH) was used to degas both the mobile phase and post-column reagent stream for all of the chromatographic studies.

Aldosterone (Sigma Chemical Co., St. Louis, MO) dissolved in acetonitrile was used to prepare a  $1.0 \times 10^{-4}$  M solution.

37% Formaldehyde (Fisher Scientific, Pittsburgh, PA) was diluted with acetonitrile to prepare a  $1.0 \times 10^{-2}$  M stock solution.

Acetaldehyde, propionaldehyde, butyraldehyde, and valeraldehyde (Aldrich Chemical Co., Milwaukee, WI) were diluted with acetonitrile to prepare individual solutions with a concentration of  $1.0 \times 10^{-2}$  M.

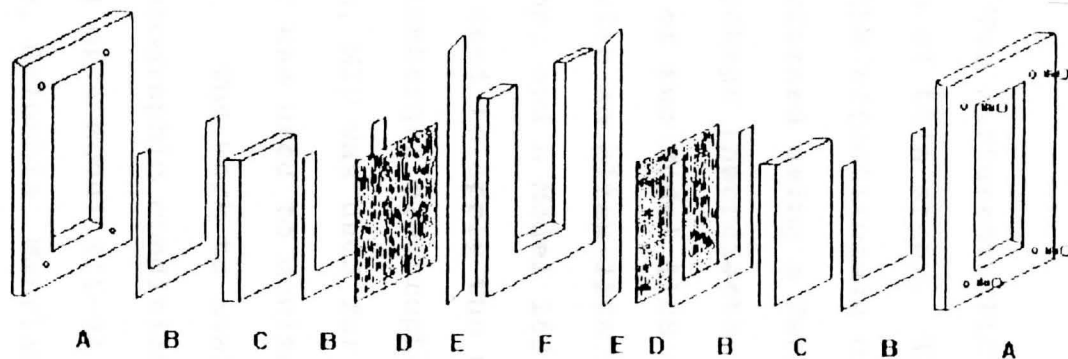
#### B. Electrochemical Studies

Cyclic voltammetry studies were performed in quiescent solutions with a supporting electrolyte of chromatographic mobile phase, which contained a 40:60 mixture of 0.2 M sodium perchlorate and acetonitrile mixed with the reagent solution in a 1:1 ratio. A nickel electrode was made in the laboratory by embedding a 5 cm x 6 mm nickel rod in epoxy. The surface was polished to a mirror bright finish. A platinum wire served as the auxiliary electrode. All potentials were measured with respect to a Ag/AgCl reference electrode. A model CV-27 potentiostat (Bioanalytical Systems, Inc., West Lafayette, IN) coupled to an Omnigraphic series 200 X-Y recorder was used in all cyclic voltammetry experiments.

A schematic drawing of the sandwich-type optically transparent electrochemical cell used to conduct the spectroelectrochemical experiments is shown in Figure 12. Two quartz windows were held in place by two stainless steel IR windows holders. The optically transparent working and auxiliary electrodes were made from nickel microscreen with 80 wires/inch (Buckbee-Mears Co., St. Paul, MN) and held against the window using a U-shaped piece of parafilm. Electrical contact to each electrode was provided by a 5 mm x 10 mm piece of copper foil placed against the electrode surface. A 0.5 cm thick piece of U-shaped parafilm was used to separate the electrodes and provide a cavity with a volume of 750  $\mu\text{L}$  and a path length of 5.0 mm.

Because the cavity was small, a miniature reference electrode was constructed. A 2.54 cm silver wire was fused in the tip of a Pasteur pipet and filled with Ag/AgCl. A 10 cm piece of Ag/AgCl wire was suspended in the filling solution and the electrode capped. The electrode tip was placed in the cell deep enough to come in contact with the sample solution yet not obstruct the light path. The same supporting electrolyte used in the cyclic voltammetric studies was used for this work.

All spectroelectrochemical experiments were performed with a model BAS CV-1B potentiostat (Bioanalytical Systems, Inc., West Lafayette, IN). The potentials were monitored in all experiments by a Radio Shack Digital



- |                     |                          |
|---------------------|--------------------------|
| A. IR Window Holder | D. 80 Line Nickel Grid   |
| B. Parafilm         | E. Copper Foil           |
| C. Quartz Windows   | F. Parafilm 0.5 cm thick |

**Figure 12**

Schematic Drawing of Spectroelectrochemical Cell Design

Multimeter. A Model 8452A Diode Array Spectrophotometer (Hewlett-Packard, Palo Alto, CA) was used for all absorption measurements.

### C. Chromatographic Studies

Two different HPLC systems were used throughout the course of this study. The preliminary studies to evaluate the effectiveness of electrochemical reactors A and B were performed using a Beckman System Gold chromatographic system (Beckman Instruments, Inc., Fullerton, CA), which consisted of two Model 110B solvent delivery modules, one equipped with an Altex 210A injection valve with a 20  $\mu$ L sample loop, and a Model 168 diode array detector. The BAS CV-27 was used to apply the potential to reactor A and a Heath-Schlumberger electrophoresis power supply (Heath Co., St. Joseph, MI) was used for reactor B. A digital multimeter was used to monitor the current.

The work to evaluate reactor C and to optimize the chromatographic conditions was done using an HPLC system consisting of a Model SIL-9A Autosampler (Shimadzu Scientific, Columbia, Maryland), a Model 2300 isocratic pump (ISCO) connected by a tee joint to a Model 600 ternary pump and a Model PDA 990 photodiode array detector (Waters Division of Millipore, Milford, MA). The column, a 250 mm X 4.6 mm I.D. 5  $\mu$  Adsorbosphere UHS C<sub>18</sub>, (Alltech Associates,

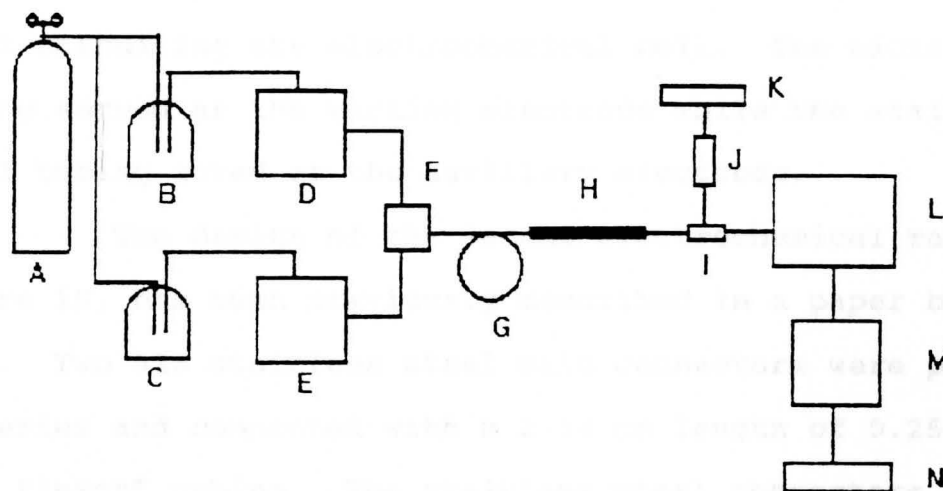
Deerfield, IL), was maintained at room temperature. The mobile phase and reagent solution were prepared fresh and filtered daily. Both were degassed with helium during operation. A 60:40 mixture of 0.2 M sodium perchlorate and acetonitrile served as the mobile phase. The reagent solution was prepared by dissolving 0.05 M Purpald in 1 M NaOH. The flow rate was maintained at 0.5 mL/min for both mixtures. A three meter length of 0.25 mm i.d. Flexon® tubing (Alltech Associates, Deerfield, IL) knitted through a plastic screen served as a mixing coil. A Fisher Scientific (Pittsburgh, PA) hotplate was used to maintain a constant temperature water bath. The BAS CV-1B was used to apply the potential to the electrochemical cell for this chromatographic system. All potentials were measured with respect to a Ag/AgCl reference electrode. A schematic diagram of the HPLC system is shown in Figure 13.

#### D. Electrochemical Reactor Design

Schematic drawings of the three electrochemical reactors investigated are shown in Figures 14, 15, 16.

The reactor in Figure 14 was constructed by connecting a 10 cm length of 0.25 mm nickel 200 tubing (Alltech Associates, Deerfield, IL) to a 10 cm length of 0.18 mm 316 stainless steel. The ends of the tubing were joined by 0.87" Delrin® flangeless nuts, Tefzel®, and a





- A. UHP Grade Helium
- B. Mobile Phase Reservoir
- C. Reagent Solution Reservoir
- D. Mobile Phase Pump
- E. Reagent Phase Pump
- F. Mixing Tee
- G. Reaction Mixing Coil
- H. Adsorbosphere UHS C<sub>18</sub> Column
- I. Electrochemical Reactor
- J. Digital Multimeter
- K. CV-1B Potentiostat
- L. Photodiode Array Detector
- M. Data Collection Station
- N. Printer

Figure 13

Schematic Drawing of HPLC System

Teflon® union fitting. When the connection was made, caution was taken so as not to allow the ends of the tubing to come into contact. This small gap was created to prevent short-circuiting the electrochemical cell. The nickel tubing served as the working electrode while the stainless steel tubing acted as the auxillary electrode.

The design of the second electrochemical reactor, Figure 15, has been previously described in a paper by Mike [39]. Two 316 stainless steel male connectors were placed in series and connected with a 2.54 cm length of 0.25 mm I.D. Flexon® tubing. The stainless steel connectors were not of the zero dead volume type. The electrode material was packed inside a cavity measuring 1.0 mm X 5.0 mm within the connector. A 0.81 mm thick 316 stainless steel frit with a porosity of 2  $\mu$  was placed inside the connector followed by nickel powder. The connector was tapped gently during addition of the nickel powder. Tight packing was avoided to prevent high backpressure that would result in rupture of the Flexon® lines. The electrode was repacked daily.

The final electrochemical reactor investigated is shown in Figure 15. The body of the cell was commercially available detector (Waters Division of Millipore, Milford, MA) [51]. The cell body was constructed of 316 stainless steel which served as the auxillary electrode. A Ag/AgCl reference electrode fit inside a Teflon® insert with a

Vycor® frit at the bottom. The working electrode was made in the laboratory by embedding a piece of 99% pure nickel shot, with a diameter of 0.4 mm, in an epoxy matrix. The electrode was polished to a mirror bright surface. A gasket with a thickness of 50  $\mu\text{m}$  separated the working and auxillary electrodes.



Figure 14

Schematic Drawing of Electrochemical Reactor

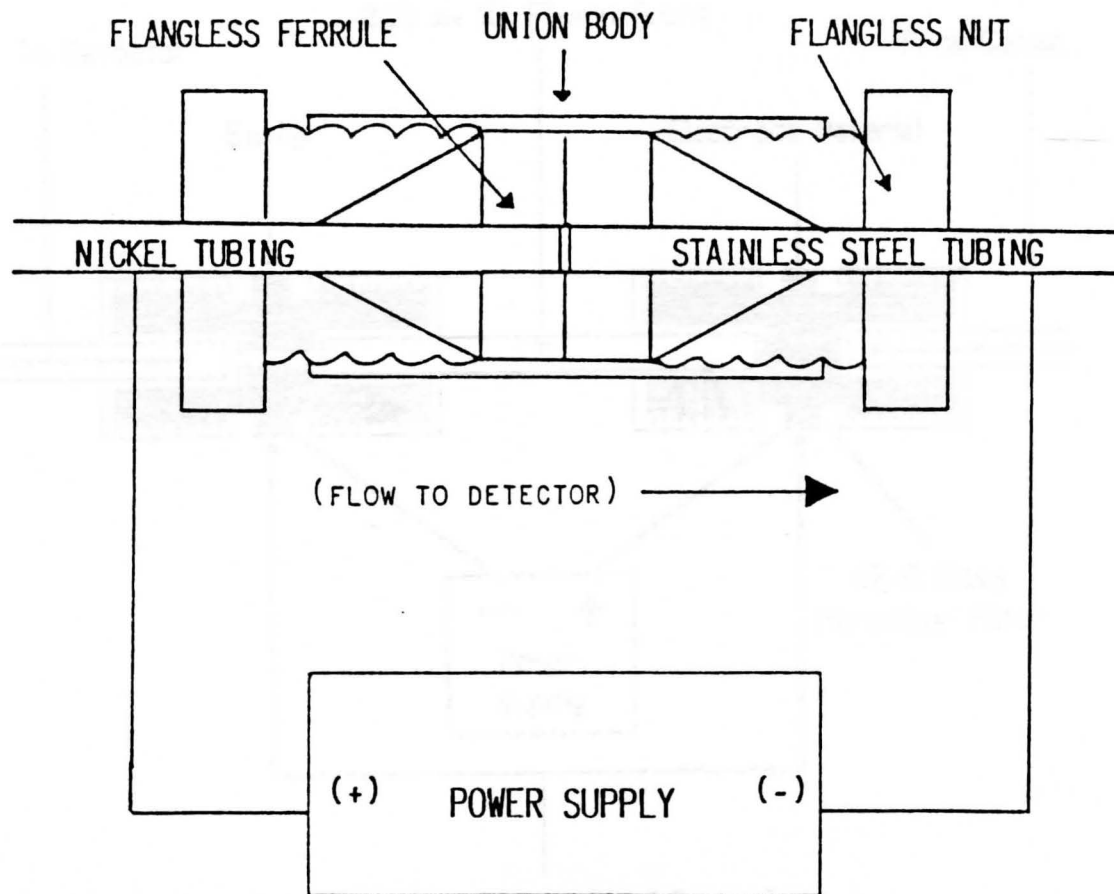


**Figure 14**

Schematic Drawing of Electrochemical Reactor A

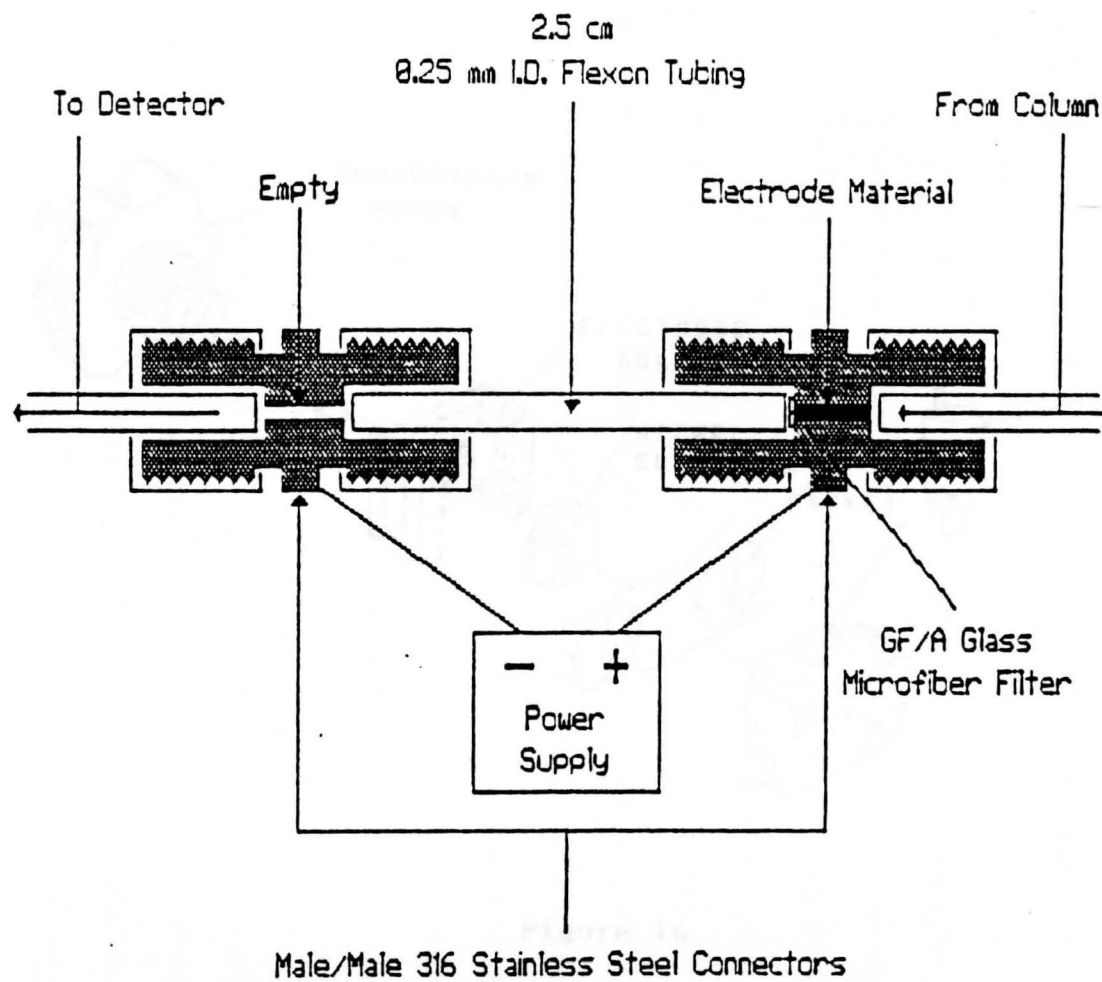


Figure 15

Schematic Drawing of Electrochemical Reactor B  
(from Ref. 39. Reproduced with permission)

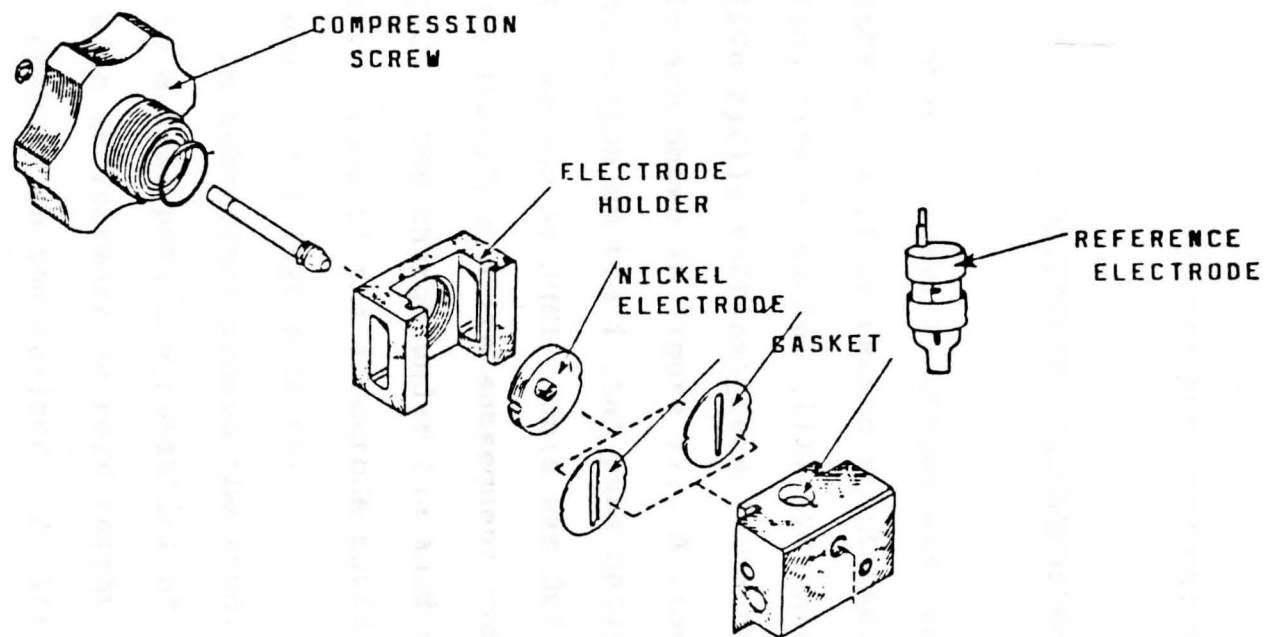


Figure 16

Schematic Drawing of Electrochemical Reactor C [50]

## CHAPTER IV

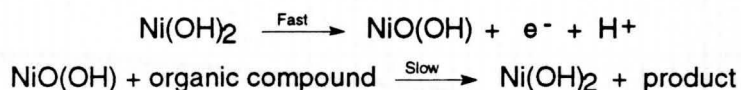
## RESULTS AND DISCUSSION

A. Electrochemical Characterization

When a nickel electrode was immersed in a solution of 1 M NaOH the surface became spontaneously covered with a passivating film of nickel (III) hydroxide [40,41]. Consecutive cyclic voltammograms for a freshly polished electrode are shown in Figure 17. A linear sweep in an anodic direction on the initial pass showed an oxidation wave at +0.43 V versus Ag/AgCl. This was due to the oxidation of  $\text{Ni(OH)}_2$  to  $\text{NiO(OH)}$  and its subsequent reduction back to  $\text{Ni(II)}$  [42]. The charge under the anodic wave indicated that the coverage of the electrode surface with the  $\text{NiO(OH)}$  species was 1 or 2 layers thick.

On subsequent passes the anodic wave gradually shifted to a less positive potential of +0.38 V versus Ag/AgCl with an increase in peak height indicating an absorbed species on the surface. As the potential was cycled the charge under the wave stabilized indicating a steady state at the electrode surface. The waves in the steady state voltammogram correspond to a one-electron reversible reaction between  $\text{Ni(OH)}_2$  and  $\text{NiO(OH)}$ .

The addition of aldosterone to the supporting electrolyte, Figures 18 and 19, changed the shape of the anodic wave considerably while the cathodic wave remained in almost the same position prior to adding the aldosterone. This type of behavior was indicative of organic compounds being oxidized by the following mechanism,



not by direct electron transfer. Fleishman et al. found this to be true for oxidation of a large group of alcohols and amines at a nickel oxide electrode [7]. This same observation was made with the addition of formaldehyde in the laboratory. The potential at which all of these organic compounds oxidize was the same, and was equal to the potential at which  $\text{Ni}^{+2}$  was oxidized to  $\text{Ni}^{+3}$ .

The cyclic voltammetry studies described above were conducted in bulk solutions of the mobile phase and the reagent phase in a 1:1 ratio using the three electrode systems previously described. The applied potential was cycled between 0.0 V and +0.5 V versus a Ag/AgCl reference electrode. The oxidation of the supporting electrolyte showed no change in physical appearance, the solution remained colorless. Upon addition of the formaldehyde a deep purple color, indicative of the Purpald<sup>®</sup>-aldehyde reaction product, was quite obvious by visual inspection at



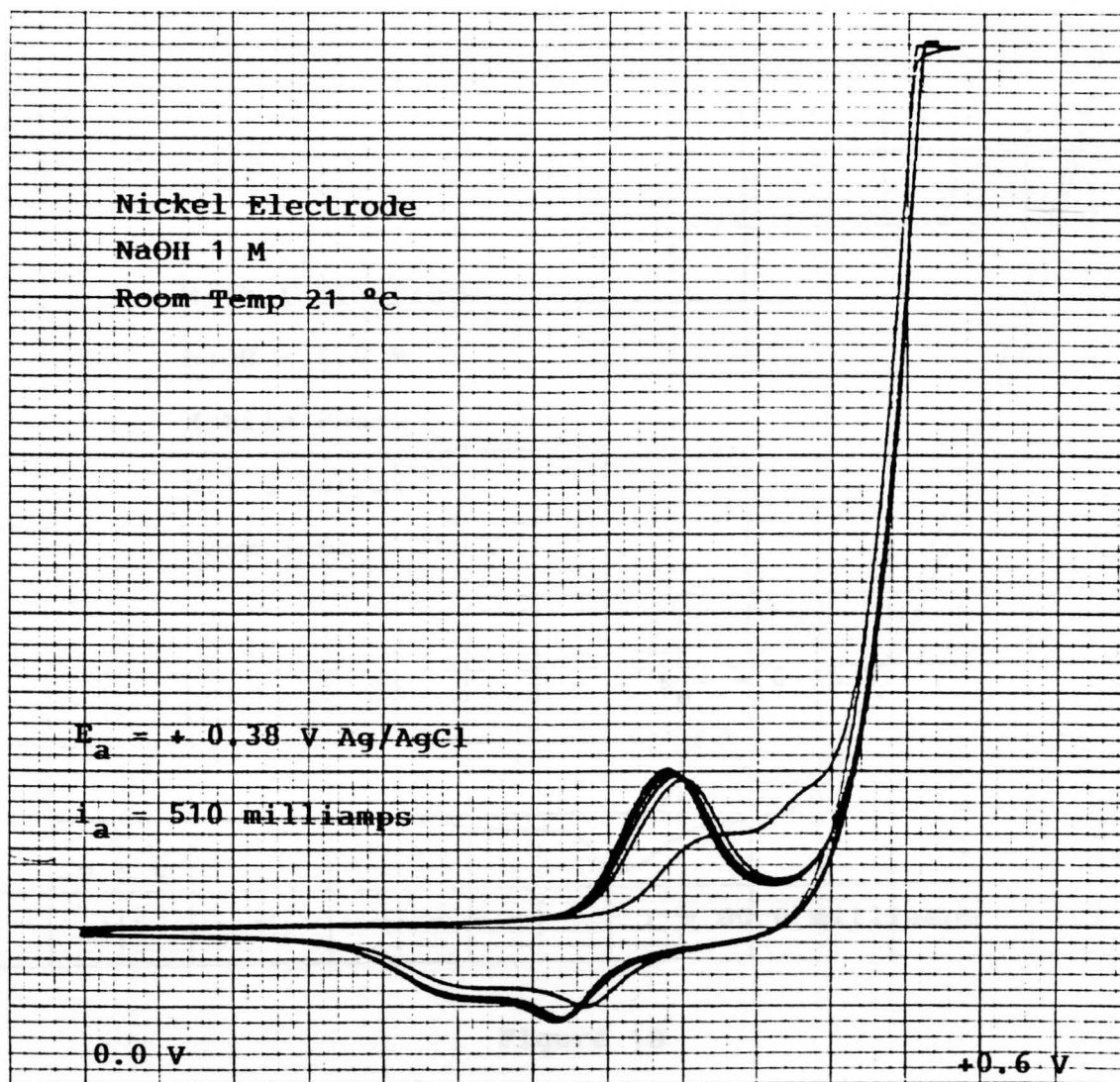


Figure 17

Steady State Voltammogram of Nickel Electrode

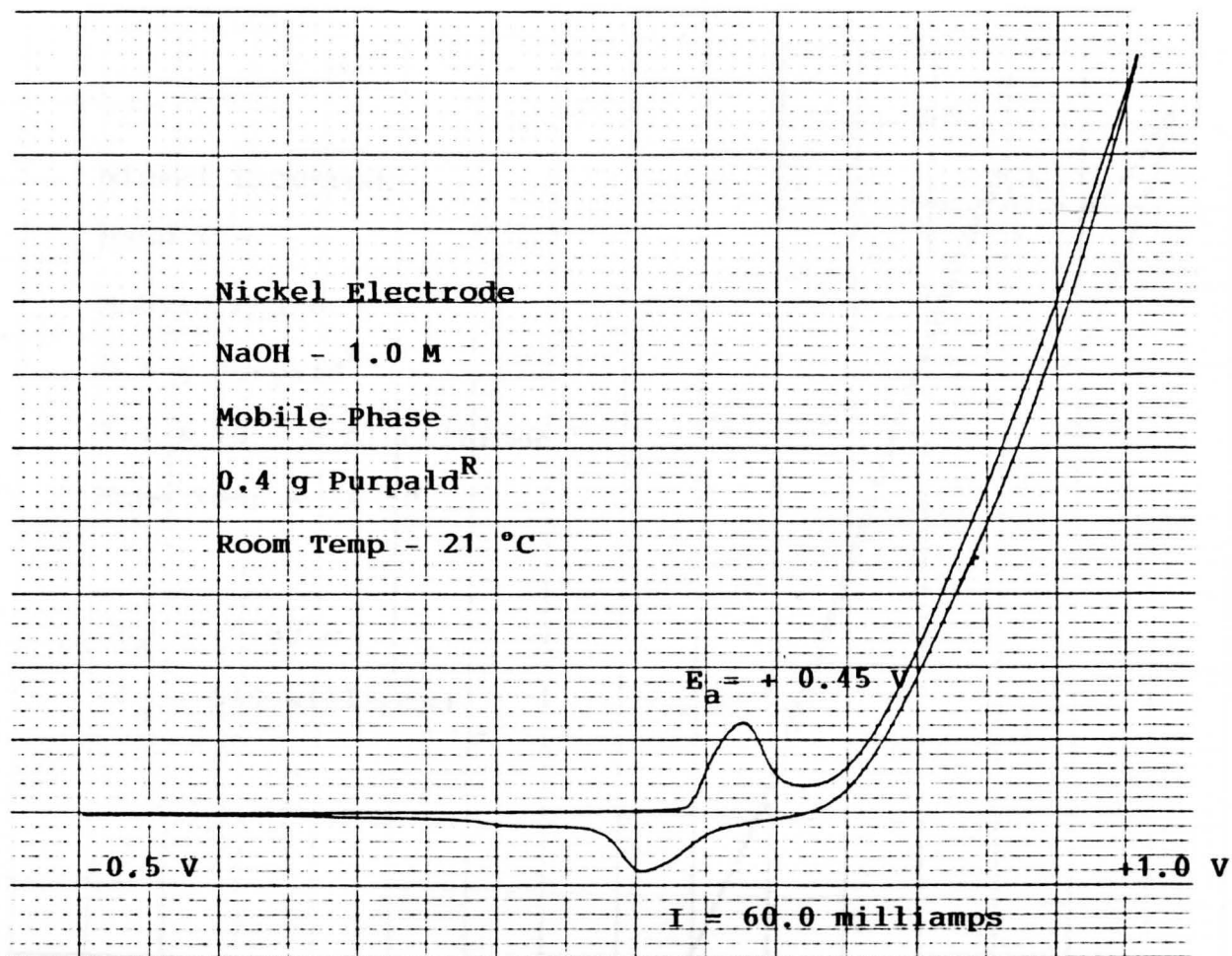


Figure 18

Cyclic Voltammogram of Supporting Electrolyte

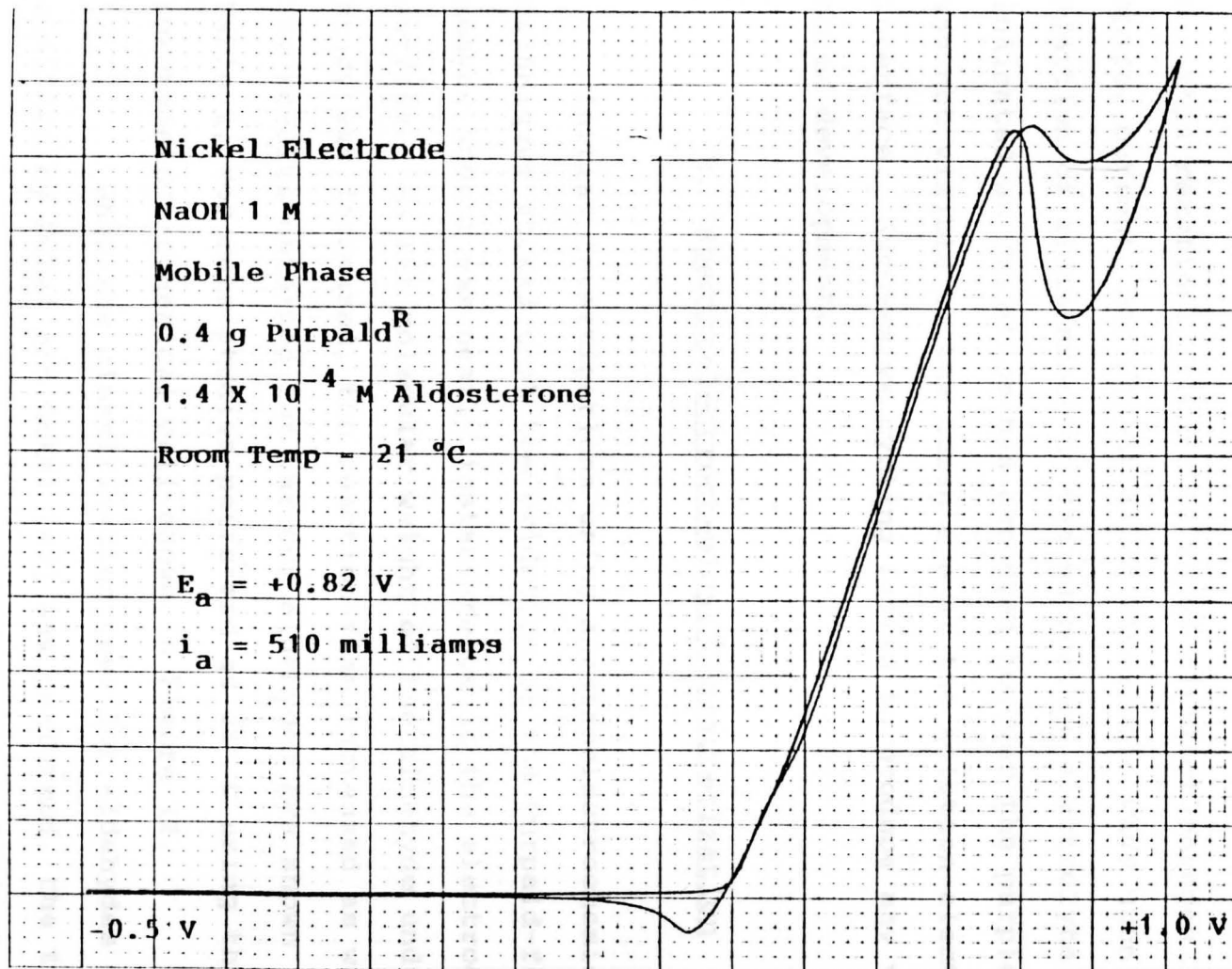


Figure 19

Cyclic Voltammogram after Addition of Aldosterone

the solution-electrode interface. The color continued to develop with successive cycling between potentials, proving that the nickel oxide electrode did indeed act as an oxidant for this reaction. Figure 19 shows distinct changes in shape, current, and potential of the anodic wave upon the addition of aldosterone to the supporting electrolyte. This indicated an oxidation had occurred however the purple color was not visible to the human eye at the solution-electrode interface. Successive cycling failed to produce any visible color development.

#### B. Spectroelectrochemical Characterization

Initial investigations using spectroelectrochemical techniques showed that the oxidation of the Purpald-formaldehyde adduct was nearly instantaneous at the electrode surface. As the molecular weight of the aldehyde under study was increased, the reaction time increased as well. The results obtained for various aldehydes are shown in Table 1, for rate studies performed at 25° C using the spectroelectrochemical cell shown in Figure 12.

When the classification test for aldehydes outlined by Durst and Gokel [43] was performed, the time required for color development was less than 5 minutes for all of the listed compounds. A possible explanation for the variation in reaction time could be the difference in NaOH

**Table 1**

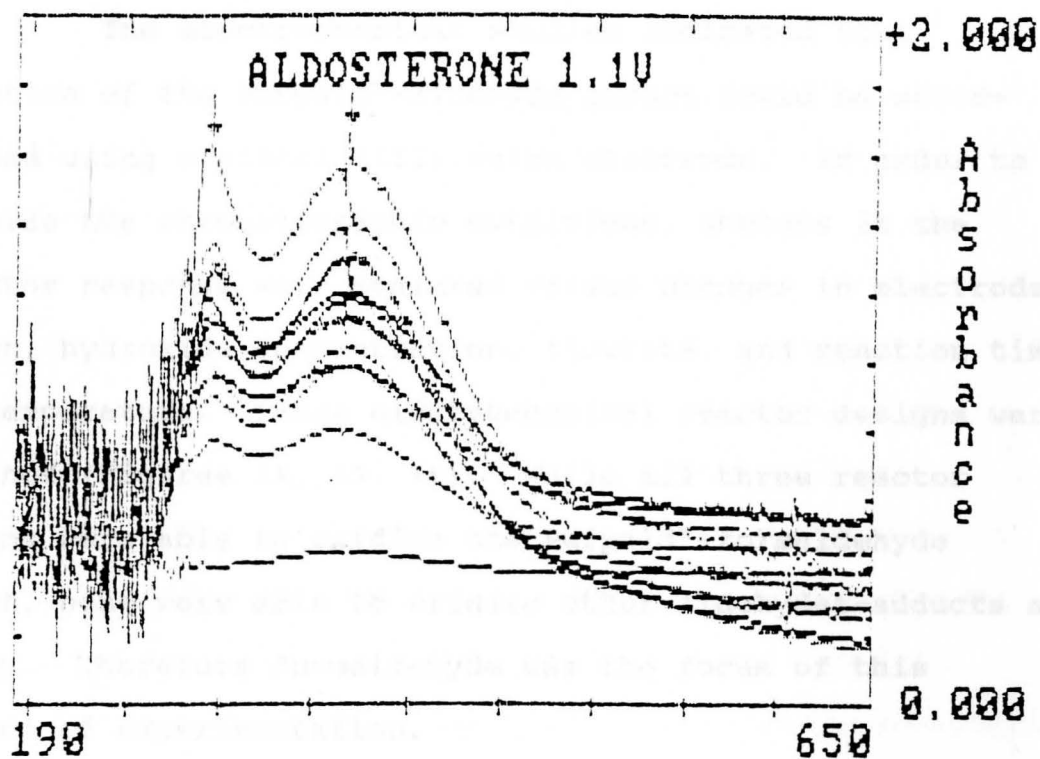
**Reaction Time for Formation of Purple  
Purpald®-Aldehyde Complex**

<u>Aldehyde</u>	<u>Reaction Time</u>
Formaldehyde	< 1 sec
Acetaldehyde	83 sec
Propionaldehyde	175 sec
Butyraldehyde	420 sec
Valeraldehyde	810 sec
Aldosterone	> 1200 sec

measured at 550 nm, at 25°C in  
a 1:1 ratio of mobile phase and  
reagent phase.

concentration. When the classification test was originally performed only 1 M NaOH was used as the solvent for the Purpald® and aldehyde. The spectroelectrochemical studies were closer to the conditions that were used in the chromatographic experiments. In this case the reagent solution containing the 1 M NaOH and 0.05 M Purpald® was diluted by 50% when it was mixed with the mobile phase at the exit of the column. It has been shown by Patrick [44] that the concentration ratio between the sample and Purpald® is critical to achieve maximum color development. Del Nozal et al. [10] also found the concentration of sodium hydroxide to be important for maximum absorbance.

In Figure 20 a peak was observed between 368 nm and 370 nm. The applied potential was +1.1 V versus Ag/AgCl, with a current greater than 19 mA. The peak was first evident when a voltage of +0.5 V was applied. The color of the solution changed from colorless to yellow. This peak was also observed during the chromatographic studies. The same yellow color was also observed upon addition of H<sub>2</sub>O<sub>2</sub>, to a solution of Purpald® [53]. It is likely that was due to an unknown oxidation product of Purald® itself, not the Purpald®-aldehyde adduct (II) shown in Figure 1. This peak appeared regardless of whether aldehydes were present or absent, and appeared when the applied potential was high. The identity of this oxidation product should be investigated in the future.



Annotated Wavelengths:

1 : Lambda = 264	Time = 100	Result = 1.62574
2 : Lambda = 369	Time = 100	Result = 1.65531

Figure 20

Spectroelectrochemical Examination of Purpald<sup>R</sup> at 21° C. Voltage measured against a Ag/AgCl reference electrode. 1:1 ratio of mobile phase to reagent solution.  $10^{-4}$  M Aldosterone solution.

### C. Optimizing Chromatographic Conditions

The electrochemical studies indicated that oxidation of the Purpald®-aldehyde adduct could be accomplished using a nickel (III) oxide electrode. In order to optimize the chromatographic conditions, changes in the detector response were measured versus changes in electrode design, hydroxide concentration, flowrate, and reaction time and temperature. Three electrochemical reactor designs were examined (Figures 14, 15, 16). While all three reactor designs were able to oxidize the Purpald®-formaldehyde adduct, none were able to oxidize other aldehydes-adducts as easily. Therefore formaldehyde was the focus of this section of experimentation.

As the cell design became more sophisticated the absorbance at 500 nm increased as seen in Figures 21, 22, 23. The maximum response was achieved using the three electrode system of the Waters electrochemical cell. By using this design the applied potential was easier to control. One significant difference between the three designs was the surface area of the working electrode, with reactor A having the smallest amount and reactor C the largest. In reactor A the surface of the electrode was the end of a piece of nickel tubing with an outer diameter of 1.59 mm an inner diameter of 0.25 mm and nominal wall thickness was 0.67 mm. By comparison reactor C had an



electrode diameter 4 mm. Since the detector response was greatest for reactor C it was used to continue the study.

The combination of the applied potential, the temperature, the reaction time, the NaOH concentration and the flow rate all had a significant effect on the detector response. An arbitrary starting point was chosen for each variable examined, then each variable was changed accordingly. The one variable that had the greatest effect on the detector response was the concentration of NaOH. Initial investigations were conducted using a concentration of 1M NaOH. A ten-fold decrease in concentration caused a significant loss in response, regardless of the applied voltage. Del Nozal et al. [10] found the NaOH concentration to be a critical factor for maximum absorbance in their study of post-column derivatization of monosaccharides using Purpald® and these results support his findings. Also, lowering the concentration of the supporting electrolyte lowered its ionic strength which directly translated to a decrease in current through the cell. Once the NaOH concentration was restored to the starting value of 1 M the absorbance increased. The presence of hydroxide is necessary for formation of the active NiO(OH) surface. Fleischmann et. al. found that the charge on the electrode surface increased with increasing hydroxide concentration [7]. The maximum charge on the electrode prior to oxygen evolution indicated that the

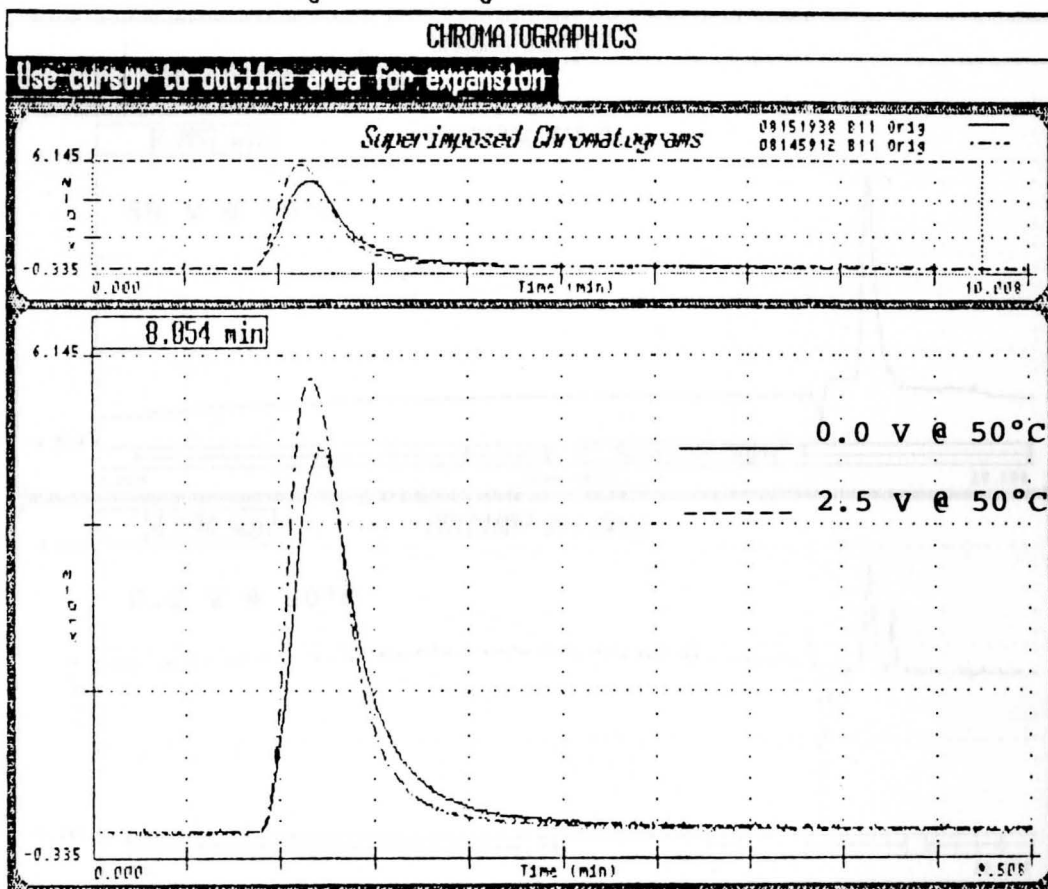


Figure 21

Oxidation of  $10^{-4}$  M Formaldehyde  
with electrochemical reactor A.  
Voltages versus Ag/AgCl

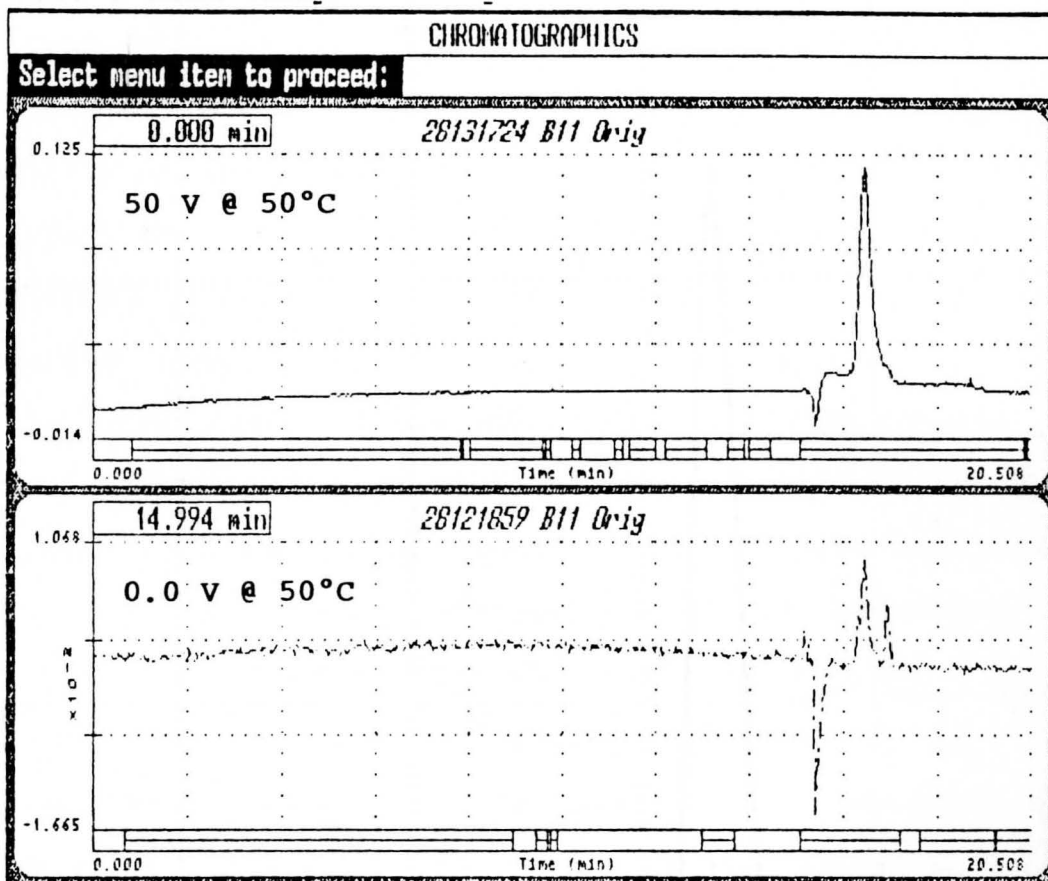


Figure 22

Oxidation of  $10^{-2}$  M Formaldehyde with electrochemical reactor B. Voltages versus Ag/AgCl.

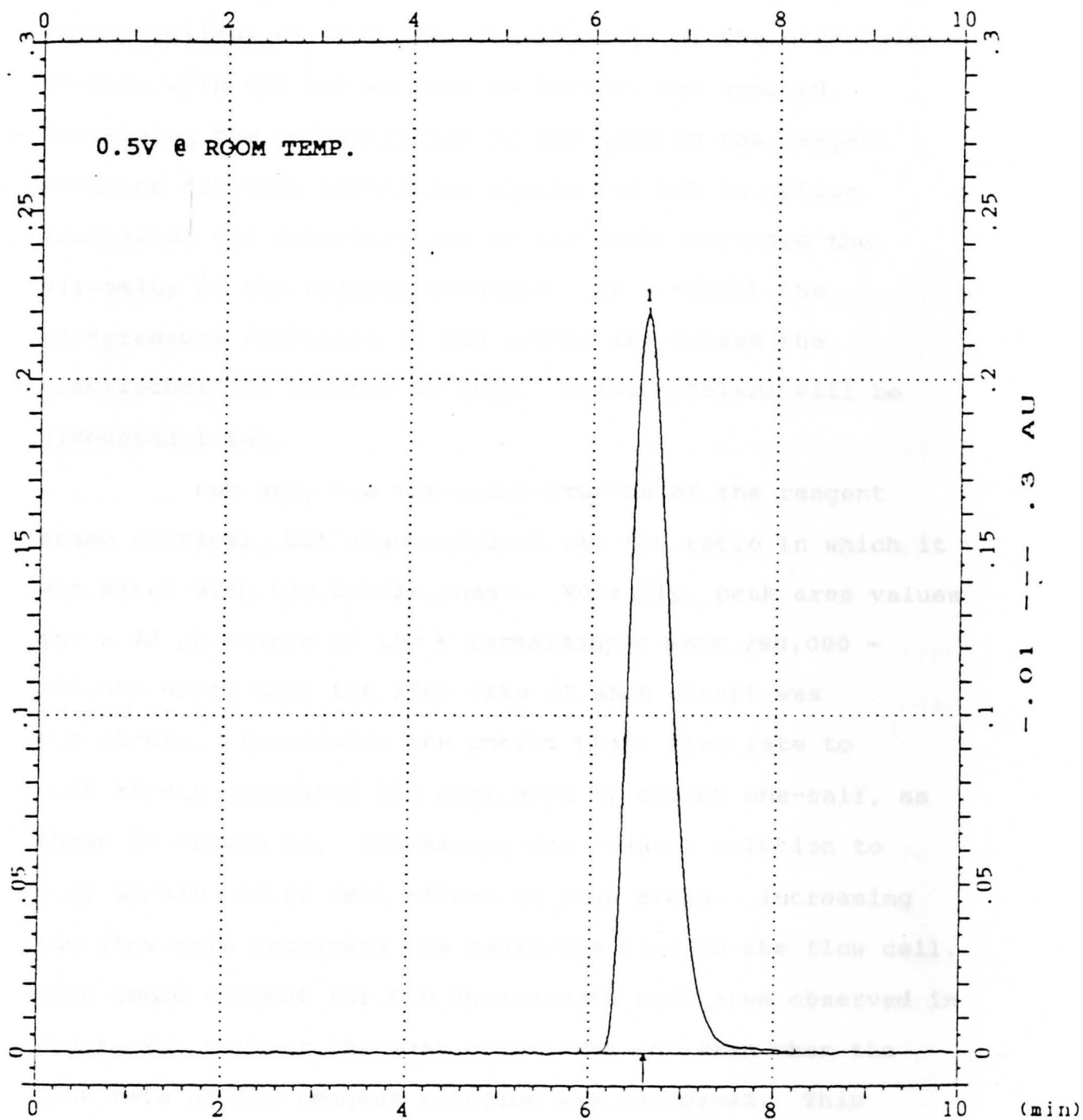


Figure 23

Oxidation of  $10^{-2}$  M Formaldehyde  
with electrochemical reactor C

NiO(OH) species had been formed. By maintaining higher concentrations of NaOH complete coverage of the electrode surface with the active form of NiO(OH) was assured. Increasing the concentration of the NaOH in the reagent solution for this particular system was not an option. Increasing the concentration of the NaOH increased the viscosity of the reagent solution. As a result the backpressure increased in the system and caused the electrochemical reactor to leak. These problems will be discussed later.

Not only was the concentration of the reagent phase critical, but also critical was the ratio in which it was mixed with the mobile phase. Normally, peak area values for a 20  $\mu$ L sample of  $10^{-2}$  M formaldehyde were 290,000 - 300,000 units when the flow rate of each eluant was 0.5 mL/min. Increasing the mobile phase flow rate to 0.65 mL/min decreased the peak area by almost one-half, as shown in Figure 24. Increasing the reagent solution to 0.65 mL/min had no real effect on peak areas. Increasing the flow rate decreased the residence time in the flow cell. This could account for the decrease in peak area observed in Figure 24, however the same effect was not seen when the flow rate of the reagent solution was increased. This pointed again to the fact that NaOH concentration had a significant effect on the reaction in terms of color development.

While decreasing the Purpald® concentration below 0.05 M showed no real change in absorbance at 550 nm, increasing it to 0.1 M created excessive out-gassing in the detector and getting reliable results was impossible.

Through cyclic voltammetric studies and in published work [1-9], the optimum anodic potential when working with nickel electrodes has been found to be +0.5 V versus Ag/AgCl. Increasing the potential to +0.75 V showed no improvement, Figure 25. When the potential was raised to +1.10 V the peak areas decreased, which may have indicated a breakdown of the Purpald®-aldehyde complex.

Increasing the temperature increased the detector response. The results are shown in Figure 26 for formaldehyde and in Figure 27 for acetaldehyde. A 30°C rise in temperature did not have much effect on the observed peak area for formaldehyde, however there was a significant increase for acetaldehyde. Overall, however, the maximum absorbance for formaldehyde was 50 times greater than that seen for acetaldehyde when the concentration of both was  $10^{-2}$  M. This was also seen in Figure 28, where the peak area for formaldehyde at room temperature with no voltage applied was 3 times greater than for acetaldehyde and 7 times greater than for propionaldehyde, both at 60°C with an applied potential of +0.5 V and a concentration of  $10^{-2}$  M each. As the molecular weight of the aldehydes increased, the detector response decreased drastically. These findings

supported the spectroelectrochemical studies.

In order for this method to be of practical importance for aldehydes of higher molecular weight, increasing the amount of the colorless intermediate formed in the first step of the reaction in Figure 1 would be necessary. This might be accomplished by increasing the temperature and/or the increasing the length of the reaction mixing coil. This last option was not possible with the current reactor design.

While the electrochemical reactor from Waters, Inc., yielded the best results there was still a problem with the design. A change in the length of the mixing coil from 3 to 4 meters resulted in an increase in backpressure of 300 psi and another increase in pressure was seen when the 3 meter coil was knitted through a plastic screen as compared to looping in a circle. Knitting the mixing coil was essential to prevent excessive band broadening [45] and to maximize mixing. Also, increasing the length of the mixing coil resulted in a leakage problem between the gasket and the stainless steel cell body due to increased backpressure in the system. Also, when the backpressure increased, leakage around the Teflon<sup>®</sup> insert for the reference electrode occurred. When the pressure was greater than 3000 psi the Vycor<sup>®</sup> frit became damaged by cracking, thereby filling the reference electrode with both mobile phase and reagent solution. The cost to replace this insert

was high and damage to the frit was more likely than it first appeared. The use of larger bore tubing for the mixing coil might be an option, however it is possible that band broadening would occur, making quantitation of the chromatographic peaks difficult.

Re-designing the electrochemical cell may be required to alleviate this problem. Schieffer [46,47] described a thin-layer amperometric detector design that was simple and used a cation-exchange membrane to separate the reference electrode from the working electrode. Johnson and Larocelle [49] used a coulometric detector in conjunction with forced-flow liquid chromatography. The design was also simple and low cost.

A design detailed by Goto [49] was the simplest, and totally eliminated the use of Vycor® frits or ion exchange resins to separate the working electrode and reference electrode. A Teflon® spacer provided electrical insulation. Since bulk oxidation of solutes was the only purpose for the cell, the use of a reference was not necessary since the current was not measured [39].



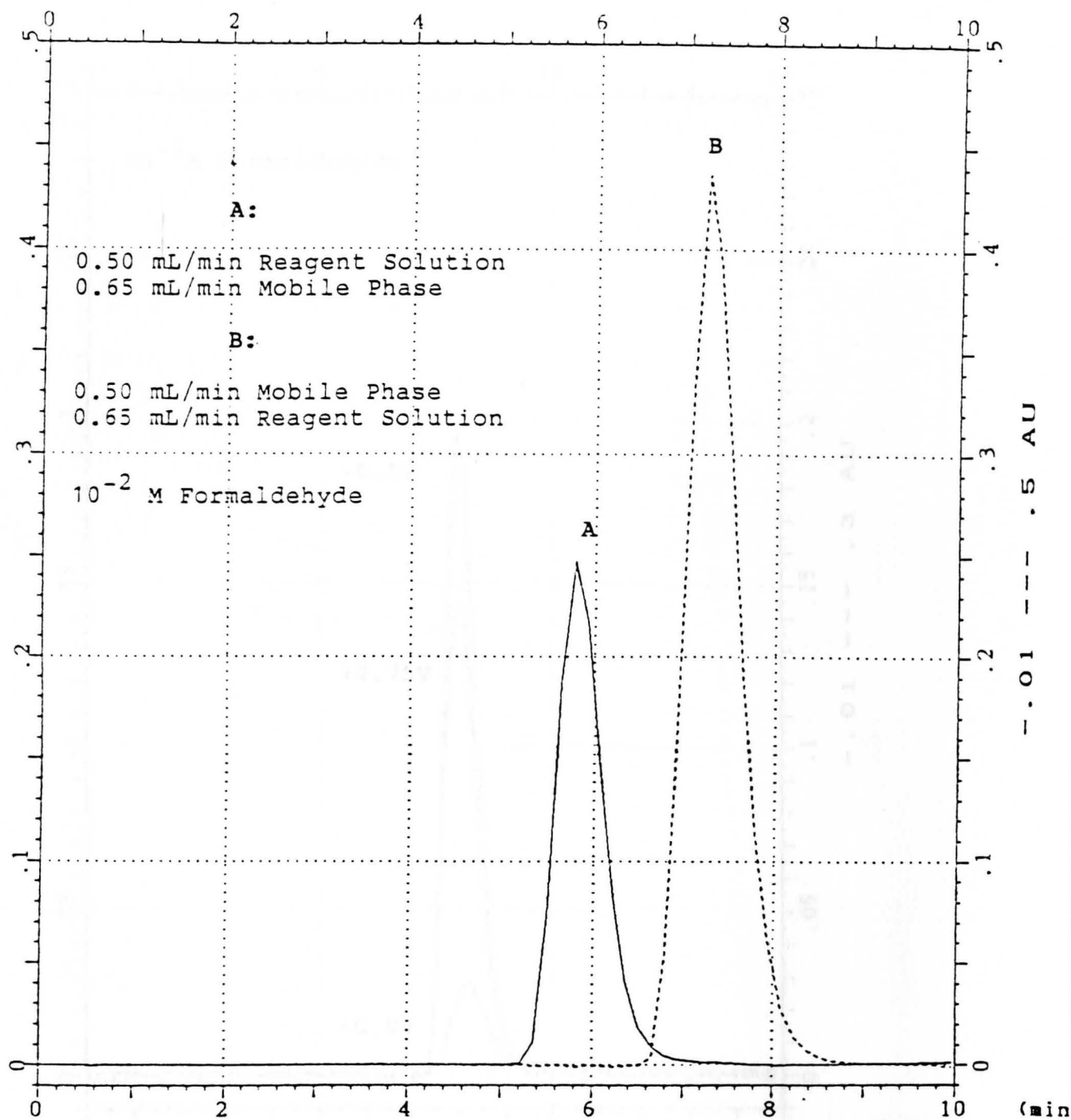


Figure 24

Detector Response with a Change in Flow Rate

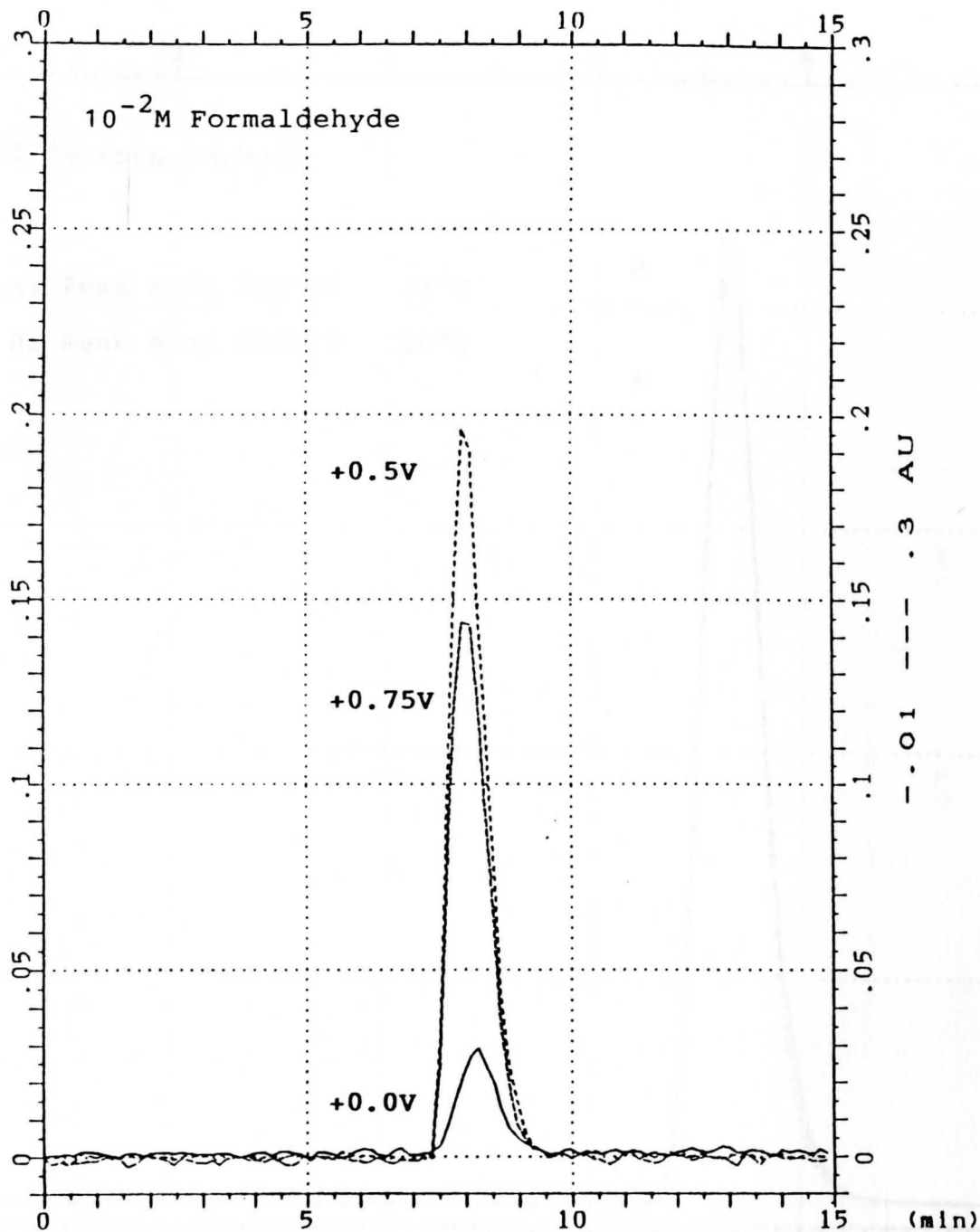


Figure 25

Detector Response with Changes  
in Applied Potential vs Ag/AgCl

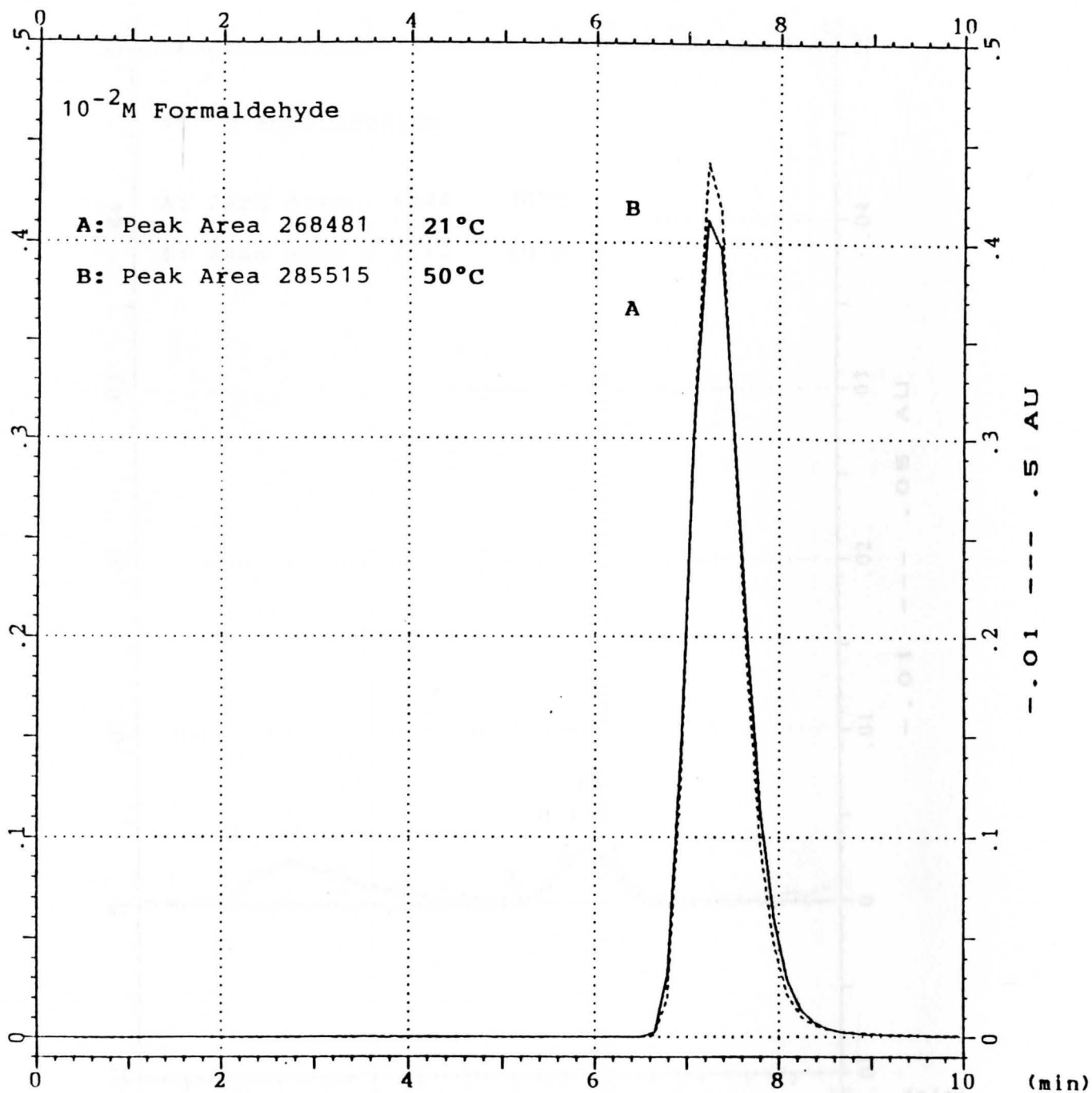


Figure 26

Detector Response with a Change in Temperature

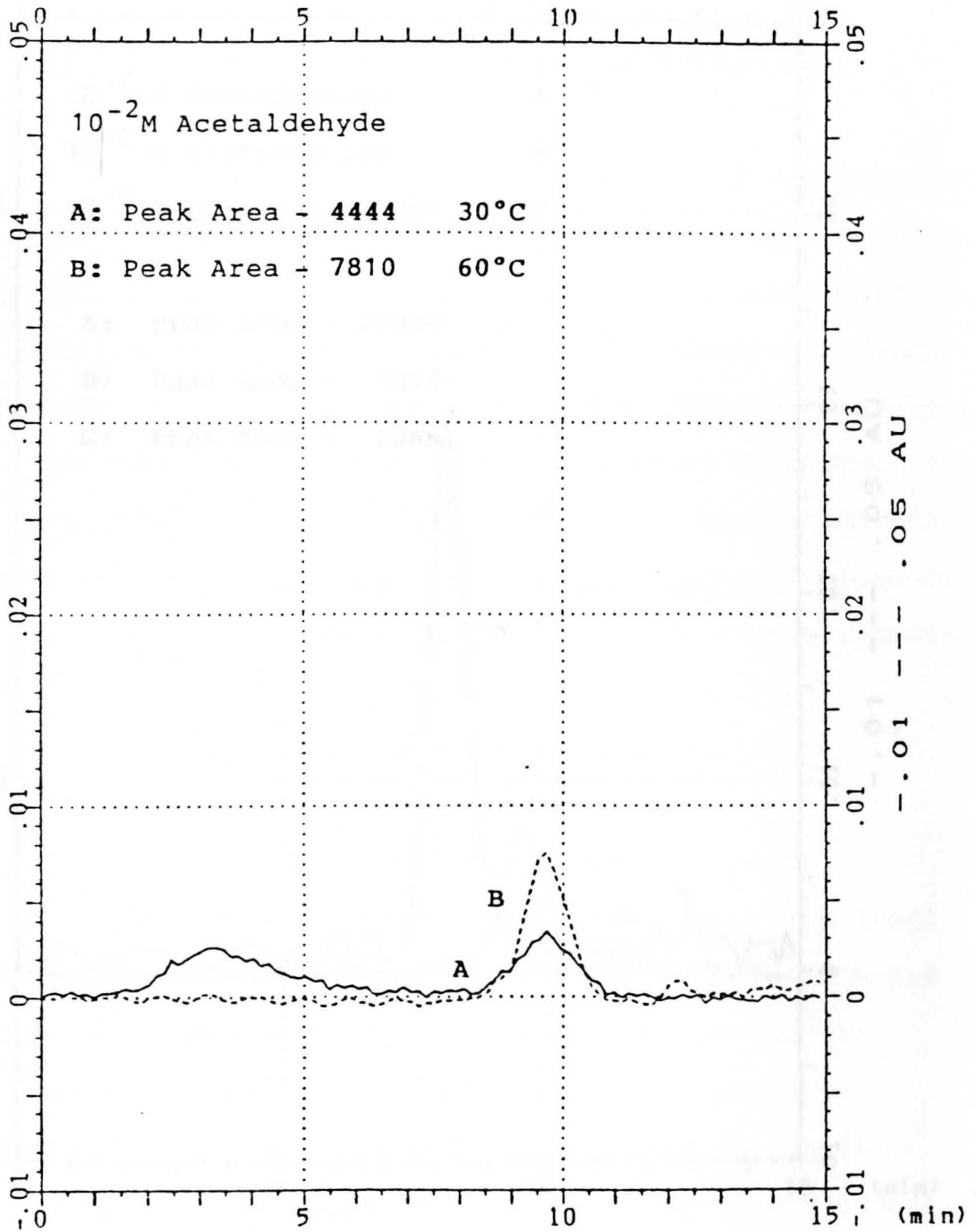


Figure 27

Detector Response with a Change in Temperature

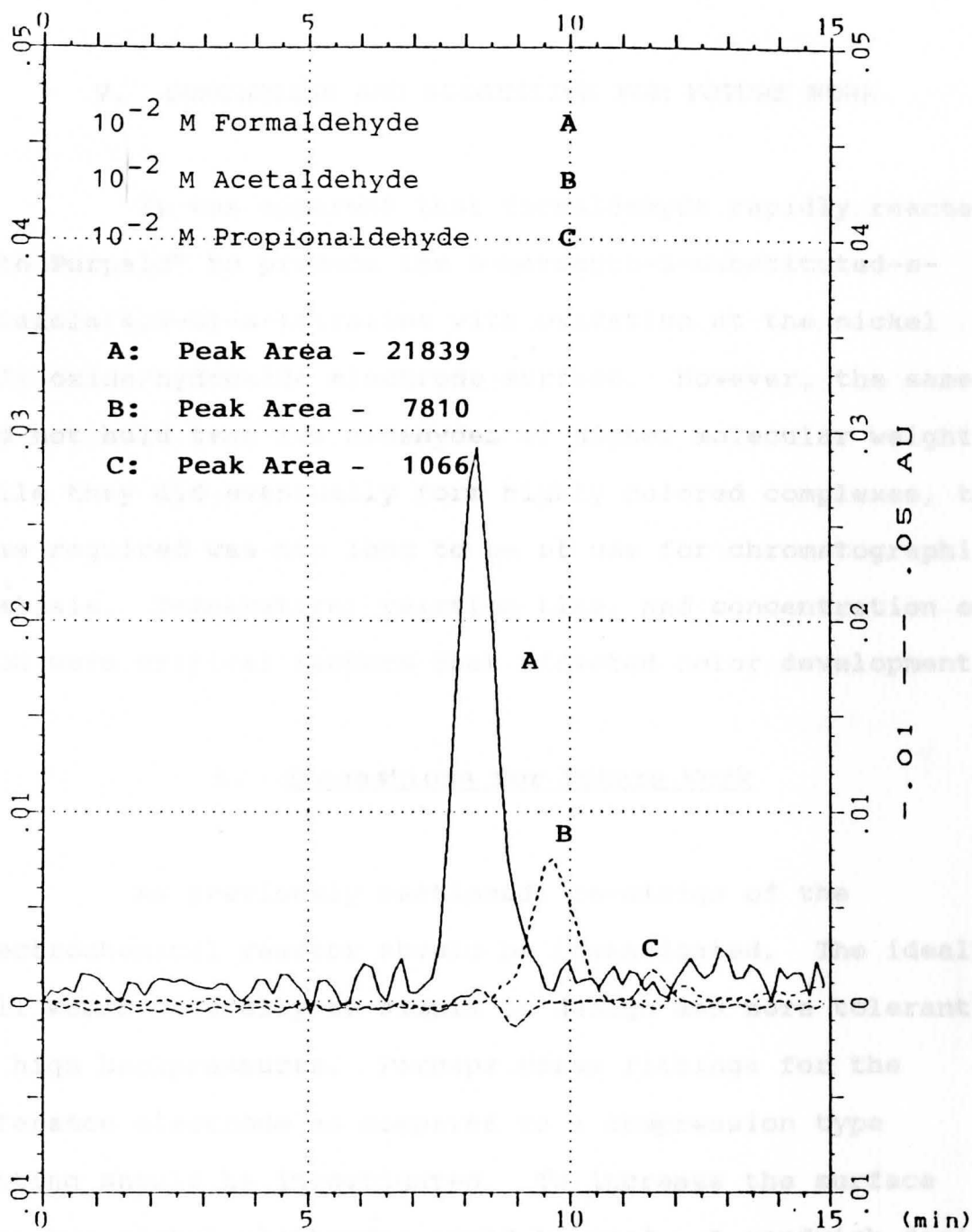


Figure 28

Detector Response versus Molecular Weight

## CHAPTER V

## V. CONCLUSION AND SUGGESTION FOR FUTURE WORK

It was apparent that formaldehyde rapidly reacted with Purpald® to produce the 6-mercapto-3-substituted-s-triazole(4,3-b)-s-tetrazine with oxidation at the nickel (II) oxide/hydroxide electrode surface. However, the same did not hold true for aldehydes of higher molecular weight. While they did eventually form highly colored complexes, the time required was too long to be of use for chromatographic analysis. Temperature, reaction time, and concentration of NaOH were critical factors that effected color development.

A. Suggestions for Future Work

As previously mentioned, re-design of the electrochemical reactor should be investigated. The ideal cell would naturally be simple in design and more tolerant of high backpressures. Perhaps screw fittings for the reference electrode as compared to a compression type fitting should be investigated. To increase the surface area two nickel electrodes could be used. A sandwich design that has both electrodes opposite to each other should be considered. Elimination of the reference electrode may be

possible. The cell design shown in Figure 15 should be re-examined. Because of the ease in which Purpald®-formaldehyde adducts can be oxidized, this simpler reactor design may be all that is necessary for quantitative studies of formaldehyde in aqueous solutions.

Much has been written concerning the proper method to condition the nickel electrode prior to analysis to maximize sensitivity [1-9]. A comparison of these results should be conducted to determine which is best for the quantitative analysis of formaldehyde.

Changing the supporting electrolyte should also be examined. Bard [51] mentions the use of LiOH and KOH improves the conductivity of the oxide film formed on the electrode surface. Some preliminary work was conducted during this study indicating that this may be true but results are limited at this point in time.

## REFERENCES

1. R. E. Reim and R. M. Van Effen, *Anal. Chem.*, 58 (1986) 3203.
2. M. Goto, H. Miyahara and D. Ishii, *J. Chromatogr.*, 515 (1990) 213.
3. J. M. Marioli, P. F. Luo and T. Kuwana, *Anal. Chim. Acta.*, 282 (1993) 571.
4. T. Ueda, R. Mitchell and F. Kitamura, *J. Chromatogr.*, 592 (1992) 229.
5. W. Buchberger, K. Winsaur and C. Breitwieser, *Frensenius Z. Anal. Chem.*, 315 (1983) 518.
6. A. Stitz and W. Buchberger, *Frensenius Z. Anal. Chem.*, 339 (1991) 55.
7. M. Fleishman, K. Korinek and D. Pletcher, *J. Chem. Soc., Perkin Trans.*, 2 (1972) 1396.
8. A. Stitz and W. Buchberger, *Electroanalysis*, 6 (1994) 251.
9. M. Fleishman, K. Korinek and D. Pletcher, *J. Electroanal. Chem.*, 31 (1971) 39.
10. M. J. Del Nozal, J. L. Bernal, V. Hernandez, L. Toribio and R. Mendez, *J. Liq. Chromatogr.*, 16 (1993) 1105.
11. R. G. Dickinson and N. W. Jacobsen, *Chem. Comm.*, (1970) 1719.
12. W. F. Evans, "Anatomy and Physiology, The Basic Principles", Prentice - Hall, New York, 1971.
13. W. F. Gonong, "Review of Medical Physiology" Lange Medical Pub., 11th ed., 1983.
14. A. White, P. Handler and E. Smith, "Principles of Biochemistry", McGraw - Hill Book Co., New York, 1973.
15. E. Glaz, "Aldosterone", Pergamon Press, New York, 1971.
16. A. Latner, "Clinical Biochemistry", W. B. Saunders, New York, 7th ed. 1975.



17. M. Griffiths, "Introduction to Human Physiology", MacMillian Pub. Co., New York, 1974.
18. H. Breuer, D. Hamel and H. L. Kruskemper, "Methods of Hormone Analysis", John Wiley & Sons, New York, 1976.
19. H. Langan, R. Jackson, E. V. Adlin and B. J. Channick, *J. Clin. Endocrinol. Metab.*, 38 (1974) 189.
20. L. Bennett, "Master's Thesis", Youngstown State University, 1982.
21. W. R. Heineman and P. T. Kissinger, *American Laboratory*, 11 (1982) 29.
22. R. D. Braun, "Introduction to Instrumental Analysis", McGraw - Hill, New York, 1987.
23. W. R. Heineman and P. T. Kissinger, "Laboratory Techniques in Electroanalytical Chemistry", Marcel Decker, New York, 1984.
24. W. R. Heineman, *Anal. Chem.*, 50 (1978) 390A.
25. T. Kuwana and W. R. Heineman, *Accounts of Chemical Research*, 9 (1976) 241.
26. L. Synder and J. J. Kirkland, "Introduction to Modern Liquid Chromatography", John Wiley & Sons, New York, 1979.
27. J. M. Miller, "Chromatography, Concepts and Contrasts", John Wiley & Sons, New York, 1988.
28. D. Knapp, "Handbook of Analytical Derivatization Reactions", John Wiley & Sons, New York, 1979.
29. C. Polo and J. Almy, *J. of Liq. Chromatogr.*, 10 (1987) 1165.
30. G. Chiavari, G. Torsi and A. M. Asmundsdottir, *Ann. Chim.*, 82 (1992) 349.
31. G. Chiavari and C. Bergamini, *J. Chromatogr.*, 318 (1985) 427.
32. G. Chiavari, C. Laghi and G. Torsi, *J. Chromatogr.*, 475 (1989) 343.
33. G. Chiavari, M. C. Facchini and S. Fuzzi, *J. Chromatogr.*, 378 (1987) 459.

34. G. Chiavari, M. C. Facchini and S. Fuzzi, *J. Chromatogr.*, 333 (1985) 262.
35. B. Mann and M. L. Grayeski, *J. Chromatogr.*, 386 (1987) 149.
36. H. Ueshiba, M. Segawa, T. Hayashi, Y. Miyachi and M. Irie, *Clin. Chem.* 37 (1991) 1329.
37. M. Katayama, Y. Masuda and H. Taniguchi, *J. Chromatogr.*, 612 (1993) 33.
38. T. Yoshitake, S. Hara, M. Yamaguchi and M. Nakamura, *J. Chromatogr.*, 489 (1989) 364.
39. J. H. Mike, B. L. Ramos and T. A. Zupp, *J. Chromatogr.*, 518 (1990) 167.
40. B. E. Conway, M. A. Sattar and D. Gilroy, *Electrochim. Acta.*, 14 (1969) 677.
41. M. A. Sattar and B. E. Conway, *Electrochim. Acta*, 14 (1969) 677.
42. J. M. Marioli, P. F. Luo and T. Kuwana, *Anal. Chim. Acta.*, 282 (1993) 571.
43. H. D. Durst and G. W. Gokel, *J. Chem. Ed.*, 55 (1978) 206.
44. M. Patrick, Youngstown State University, Chem. Dept., personal communication, 1992.
45. B. Lillig and E. Henz, "Reaction Detection in Liquid Chromatography" in "Chromatographic Science", I. S. Krull eds., Marcel Dekker, Inc., New York, (1986), vol. 34, pg. 27.
46. G. Schieffer, *Anal. Chem.* 52 (1980) 1995.
47. G. Schieffer, *Anal. Chem.* 53, (1981) 126.
48. D. Johnson and J. Larochelle, *Talanta*, 20 (1973), 959.
49. M. Goto, Y. Koyangi and D. Ishii, *J. Chromatogr.*, 208 (1981) 262.
50. "Water 460 Electrochemical Detector Operator Manual", Waters Associates, Inc., Milford, MA, 1st ed., 1986,

51. A. J. Bard, "Encyclopedia of Electrochemistry of the Elements", vol. 3, Marcel Dekker, New York, 1973.
52. R. M. Silverstein, G. C. Bassler and T. C. Morrill, "Spectroscopic Identification of Organic Compounds", 4th ed., John Wiley & Sons, New York, 1981.
53. J. H. Mike, Youngstown State University, Chem. Dept., personal communication, 1995.